REPORT DOCUMENTATION PAGE

Form Approved OMB No. 0704-0188

1. AGENCY USE ONLY (Leave Blank)	2. REPORT DATE	3. REPORT TYPE AND DATES COVERED
	3/15/98	Final 9/15/97 - 3/15/98

4. TITLE AND SUBTITLE
Real time Chemical Emissions Monitor

5. FUNDING NUMBERS
DEFG03-97ER82417

6. AUTHOR(S)
James J. Scherer

7. PERFORMING ORGANIZATION NAME(S) AND ADDRESS(ES)
Los Gatos Research

8. PERFORMING ORGANIZATION REPORT NUMBER
98-3-1

9. SPONSORING/MONITORING AGENCY NAME(S) AND ADDRESS(ES)
Department of Energy

10. SPONSORING/MONITORING AGENCY REPORT NUMBER

11. SUPPLEMENTARY NOTES

12a. DISTRIBUTION/AVAILABILITY STATEMENT

12b. DISTRIBUTION CODE

13. ABSTRACT (Maximum 200 words)

See attached Document

14. SUBJECT TERMS
Optical Diagnostics

15. NUMBER OF PAGES
50

16. PRICE CODE

17. SECURITY CLASSIFICATION OF REPORT	18. SECURITY CLASSIFICATION OF THIS PAGE	19. SECURITY CLASSIFICATION OF ABSTRACT	20. LIMITATION OF ABSTRACT

DISCLAIMER

DISCLAIMER

Portions of this document may be illegible in electronic image products. Images are produced from the best available original document.

(BLANK)

Significance and Background Information

3. Identification and Significance of the Problem or Opportunity, and Technical Approach

New technologies are needed to facilitate the successful and safe storage, remediation, and management of toxic chemical waste. Technologies capable of monitoring and determining absolute concentrations of specific waste concentrations in the gas phase can be employed to assist in the characterization as well as minimization of toxic effluents. In the latter case, the ability to monitor chemical concentrations in real time is needed for the rapid assessment of remediation process efficacy, which requires the ability to monitor transient discharges. Techniques with real-time capability can be implemented as feedback devices for optimizing processing or waste treatment methods, assaying chemical emissions levels for regulatory compliance, and monitoring the migration of ultra trace level chemical or biological plumes. Although many characterization methods currently in use have demonstrated extremely low concentration detection limits for many species, they typically suffer from long data update intervals, sophisticated calibration procedures, or must frequently be implemented in conjunction with cumbersome sampling technologies, such as chemical scrubbing or liquid sample preparation. Faster, more sensitive, and in-situ quantitative technologies are required to achieve both high sensitivity and rapid data acquisition rates.

Recent developments in optical components and spectrally bright light sources have led to a variety of laser-based chemical sensor technologies, which in some cases are capable of real-time analysis of toxic gases. One such recently developed technology currently in use for monitoring heavy metals is Laser Spark Spectroscopy (LS).[1] Although highly sensitive and suitable for monitoring the *presence* of several metals, LS is not generally capable of providing *absolute concentrations* for those species. Thus LS is not always suitable for tasks such as process optimization or emissions monitoring for regulatory compliance. Additionally, the high internal temperatures attained in LS result in broadened spectral signatures, which in some cases degrades speciation capability. Recently, inductively coupled plasmas (ICP), which do not generate the high internal temperatures of LS, have been utilized in conjunction with conventional Atomic Absorption (AA) or Emission (EM) spectroscopies, as a means of

providing elemental concentrations.[2] However, these methods also require tedious calibration procedures (EM) or can suffer from low sensitivity (AA).

Other, more sensitive optical absorption-based detection methods have recently been employed and developed for quantitative monitoring of offgas streams, including Diode Laser Absorption Spectroscopy (DLAS)[3] and Fourier Transform Spectroscopy (FTS). Frequency or wavelength modulated DLAS, although commonly employed to enhance detection sensitivity in some environments, can be difficult to implement in spectrally congested areas and is primarily limited to near to mid-infrared spectral regions.[4] Thus, DLAS is unsuitable for monitoring many waste species such as metals, which are readily identified by their atomic spectral signatures in the ultraviolet. Similarly, FTS, which is not as sensitive as methods such as DLAS, is generally limited to visible and infrared spectral regions. Moreover, these traditional absorption based methods require slow scanning of the input laser, or moving of the interferometer optics, resulting in relatively slow (> minutes) data update intervals for all but extremely narrow wavelength regions.

Recently, Cavity Ringdown Laser Absorption Spectroscopy (CRLAS) has been developed and demonstrated to be an extremely sensitive and robust spectroscopic tool in a variety of environments, applications, and spectral regions (200 nm-4.5 μm).[5,6,7] Recently, CRLAS has been implemented for studies with ICP sources, and exhibits similar performance levels to those achieved in flames and molecular beams. However, to date, CRLAS has not been effectively employed as a real-time diagnostic tool, as the method requires data to be obtained over a spectral region large enough to determine absorption from other, non-resonant losses such as scattering. Thus, the technique, although extremely sensitive, typically requires scanning times of minutes. To understand this deficiency in more depth, we will briefly review the basic theory and practice of CRLAS.

In a conventional CRLAS experiment, shown in Fig. 1, narrowband laser light is coupled into a highly reflective optical cavity, and the decay or "ringdown" time of the intracavity light

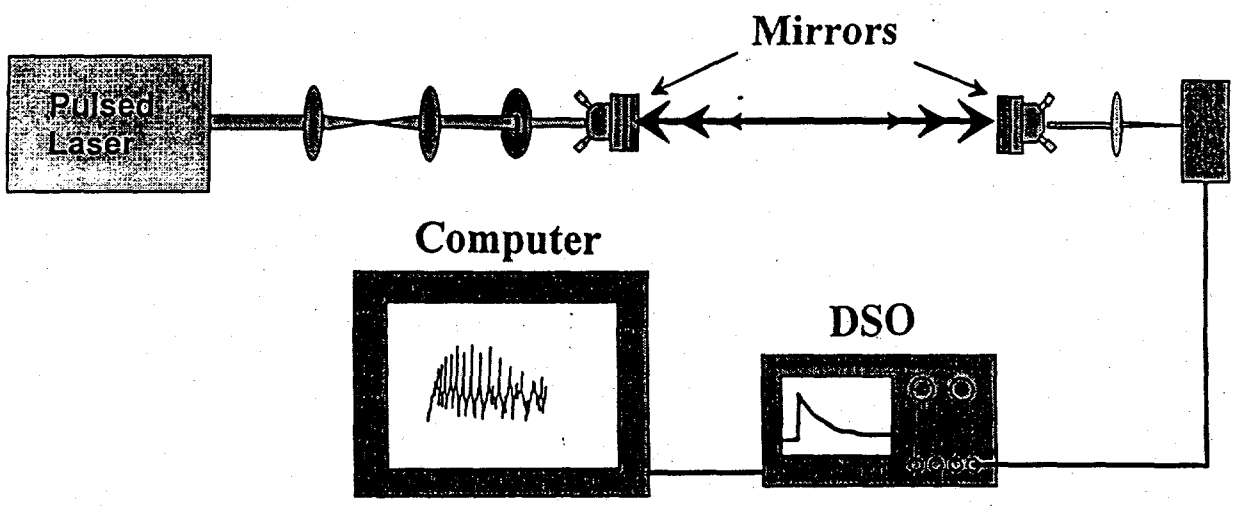

Figure 1. Pulsed CRLAS experiment: the characteristic decay or "ringdown" time of a high finesse cavity is measured using pulsed lasers and transient recorders. The ringdown time measurement allows total cavity losses per pass (including absorption) to be determined.

intensity is recorded as a function of the input laser frequency. Total per pass cavity losses are calculated from the measured decay time, and include mirror reflectivity, scattering, and absorption for species located between the mirrors. Absorption is determined by subtracting the baseline (non-resonant) losses of the cavity, which are primarily due to the finite mirror transmission and are determined while the laser is off-resonance with transitions. The power of the CRLAS method lies in the extremely high sensitivity and simplicity of the technique, together with the fact that it does not require a priori knowledge of upper state dynamics, such as is frequently required in other sensitive optical techniques such as EM. As an absorption-based method, CRLAS is highly desirable for quantitative spectral studies of trace atomic as well as molecular species, as species concentrations are easily inferred from the absorption spectra with extremely high accuracy. Detection limits for many species are in the *part-per-billion to part per trillion range.*[8]

In case where only narrow spectral regions need be covered on modest timescales, such as would be the case for detecting a single atomic species, conventional CRLAS can be employed with great success in many cases, since only a small frequency bandwidth need be covered. However, in the event that many species need be monitored, larger spectral regions *must* be

covered, and this is currently accomplished by tuning the input laser at a relatively slow rate, leading to monitoring times ranging from minutes to hours. Additionally, the need to subtract non-resonant losses from the measured total cavity losses, inherently requires wavelength scanning for even narrow spectral regions. A such, CRLAS is not suitable for real-time monitoring applications, such as those specifically sought by the DoE. What is needed in this case is a technique which is capable of acquiring quantitative absorption data in real time, from which species concentrations may be reliably deduced.

To address this need, Los Gatos Research, has invented and demonstrated a powerful new diagnostic technology which will allow *absolute concentrations of multiple species to be monitored on a microsecond time scale*. The results of our Phase I research on Broadband Ringdown Spectroscopy (BRS in the Phase I Proposal), which we have since renamed more appropriately as Ringdown Spectral Photography (RSP), indicate that this new technology possesses both high sensitivity as well as this important real-time capability, with an associated time resolution of microseconds.

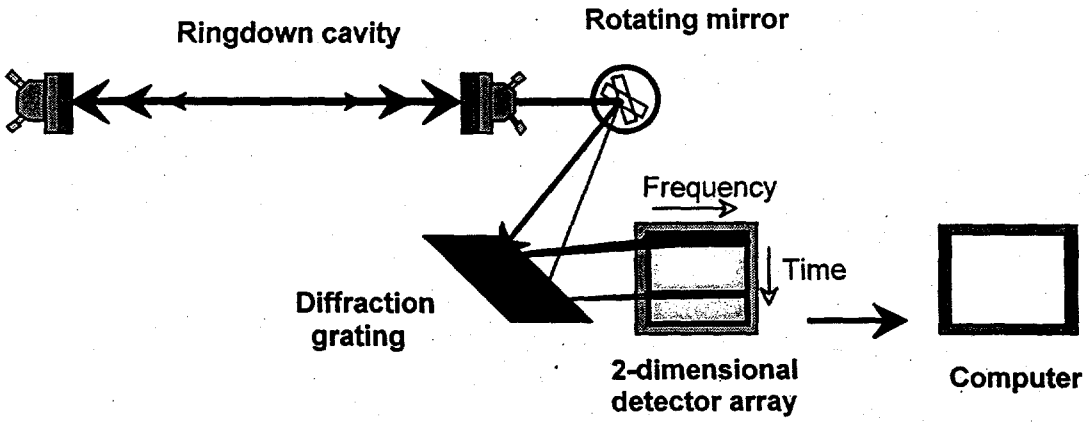

Figure 2. RSP experiment: A single ringdown event is dispersed time with a high speed rotating mirror and in wavelength with a diffraction grating. The wavelength resolved decay times are recorded with a 2-dimensional array, and the entire absorption spectrum is calculated after downloading the channels to a PC.

A simplified schematic of the RSP method is shown in Fig. 2. Broadband laser light is coupled into a two mirror optical cavity and detected outside the exit mirror with a rapidly

rotating mirror, diffraction grating, and multielement CCD camera assembly. The firing of the laser light is synchronized with the rotating mirror such that the decaying intracavity light intensity is spatially deflected along a single axis of a (CCD) array. Simultaneously, the light is separated in frequency along the other (orthogonal) axis of the array with a diffraction grating (or other dispersive element) which is placed in between the rotating mirror and camera. The decaying light intensity resulting from the photon lifetime inside the resonator is recorded as a streak trace of exponentially decaying intensity. The result for a single pulse of broadband light is a 2-dimensional image of frequency vs. time. This image can be converted to yield absorption vs. frequency by fitting the subsequent exponential rate of decay of the frequency specific (continuous) "streak" images. The result is a high resolution cavity ringdown spectrum obtained for a broad frequency range, but done so with a *single pulse* of broadband input light. This RSP approach, as we have named it, is capable of obtaining high CRLAS-level sensitivities, but with an effective scanning rate which is orders of magnitude faster than CRLAS, which requires relatively slow tuning of the input laser. As an all optical method, the RSP technology is inherently non-invasive, which enables nonperturbative, in-situ measurements to be made with the added benefit of generating no secondary waste.

In this Phase II proposal, we present the results of our Phase I research which assessed the feasibility of the fundamental concepts employed in RSP, and submit a detailed plan for the development of a higher performance Phase II prototype instrument. In the Phase II Work Plan, we will first refine the RSP apparatus, and employ the technology in conjunction with an ICP source for the specific task of heavy metal monitoring in the UV spectral region. This demonstration will establish that RSP can be employed for either emissions monitoring or process optimization in thermal waste treatment facilities. Below, the performance levels obtained in the Phase I apparatus are used to estimate routine performance levels for the Phase II RSP prototype, with associated projected performance detection limits for several heavy metal species currently relevant to Mixed Waste Focus Area (MWFA) concerns. In this proposal, we focus on the specific development of RSP for determining heavy metal concentrations via the associated atomic UV absorption spectra. However, the technology could similarly be employed as a highly sensitive monitor of molecular species such as VOC's in other spectral regions, such

as the visible or infrared. Additionally, we will address experimental issues concerning the applicability of the technology for use as a process stack monitor, including integration for process control or waste stream plume monitoring.

The successful development of RSP will enable real-time concentration data of trace toxic wastes to be obtained with extremely high sensitivity using readily available off-the-shelf hardware. As such, RSP holds great promise for further development of simple, low-cost, commercial devices. Examples of applications aside from those focused on here for the specific task of metals monitoring include the development of general analytical instrument and research tool, as the method possess several unique capabilities. The proposed RSP technology will contribute greatly to the chemical detection industry across a wide range of Federal missions and commercial markets. Below, we focus on the specific impact expected within the DoE for the specific task of offgas monitoring for chemical remediation technologies. Our Phase I research indicates that RSP is a viable new technology which can be implemented with existing off-the shelf hardware and employed as a highly sensitive chemical characterization technology, enabling chemical species to be detected in real time in many cases below the ppb concentration level.

4. Anticipated Benefits

The RSP technique will provide a fundamentally new diagnostic capability which can be employed for a wide range of DoE missions as well as commercial interests. In this section, we give examples of the potential impact in both the Federal Government as well as the commercial sector. For the former we focus on the utilization of RSP for the characterization and monitoring of heavy metals in gas streams of waste processing facilities, while in the latter we explore the commercial potential of a general analytical instrument.

Specific branches of the Federal Government Impacted by RSP

The proposed RSP development will have an immediate impact on a broad range of Federal missions. Here, we focus on the specific implementation for the DoE mission of chemical characterization and emissions monitoring. As discussed earlier, new technologies are

sought in this arena which possess real-time capability, in order to monitor remediation process efficacy as well monitor transient emissions for regulatory compliance. Chemical species of concern targeted in the Resource Conservation and Recovery Act (RCRA) include heavy metals (e.g. mercury), Volatile Organic Compounds (VOC's) such as trichloroethylene, and radionuclides such as ^{129}I. Mercury vapor is of particular concern because of its bioaccumulation toxicity, while VOC monitoring is needed for thermal treatment waste processing plants and storage facilities such as Hanford.[9] Traditional methods employed for the detection of these species are largely inappropriate for real time analysis. For example, current methods employed for the monitoring of offgas streams in thermal treatment plants typically combine cumbersome sampling techniques (such as dry filtering and chemical scrubbing) with conventional analytical methods such as Gas Chromatography (GC), and can require processing times up to hours to achieve necessary sensitivity levels.[10] As such, this approach is unsuitable for either in-situ process optimization, hazards assessment, or the remote monitoring of transient emissions.

Here, we focus on the specific application of RSP to the detection of heavy metals, although the technology is by no means limited to these species or the UV spectral regions discussed. Our initial Phase I effort established the feasibility of the fundamental concepts employed in RSP in the visible spectral region, as a proof of principle demonstration. The extension to both the UV proposed here is completely straightforward and poses no major technical barriers. Following the below discussion of sensitivity limits, the issue of the application and integration of RSP to waste characterization and remediation technologies will be addressed.

RSP Heavy Metal Monitor: Applications and Sensitivity

Current EPA methods employed for heavy metal monitoring in offgasses and plumes frequently involve isokinetic extractive gas sampling followed by extensive sample preparation and chemical scrubbing. Post-sampling analytical methods are then employed to determine the stream composition, such as mass spectrometry (MS) and gas chromatography (GC), but can require up to several hours to achieve desired sensitivities. Some of the most sensitive post

sampling methods currently employed combine conventional absorption, emission, and mass spectrometric detection with Inductively Coupled Plasma (ICP) sources.[2] These spectroscopic methods used in tandem with ICP allow total elemental concentrations to be determined by atomizing the compounds with ICP followed by gas phase detection via characteristic atomic absorption or emission spectra. To be competitive, new technologies developed for heavy metal monitoring should meet or exceed current sensitivity limits (minimum concentration limits) of existing Reference Methods and EPA Methods. In this section, we show that the detection sensitivities given by these Methods are easily met or exceeded with the proposed RSP technology. RSP can be employed as a heavy metal monitor to either measure free elemental concentrations directly in a process offgas stream or in conjunction with an ICP source as a means of determining total elemental concentration resulting from all associated compounds in the stream. In either case, the suitability of RSP as a heavy metal monitor depends on both the total number of metals which can be monitored within a specified bandwidth, and the associated minimum detectable concentration levels for these species.

~325 nm			~275 nm			~250 nm		
species	λ, nm	*f*	species	λ, nm	*f*	species	λ, nm	*f*
Ag	328.07	0.451	**Ni**[b]	274.67	0.0013	***Hg***	*253.65*	*0.0042*
Ni	323.29	0.014	**Fe**	271.90	0.12	**Fe**	252.23	0.28
Sc[a]	327.36	0.286	**Mn**	279.48	0.57	**Co**	252.14	0.23
V	326.32	0.017	**Sc**[c]	271.14	0.29	**Ni**	247.69	0.0018
						Ti	252.05	0.022

-a, b, and c transitions originating from low lying levels 168 cm^{-1}, 204 cm^{-1}, and 108 cm^{-1}, respectively, above their associated ground states.

Table 1. Atomic transitions and associated oscillator strengths for three narrow spectral regions in the UV. These transitions all originate in the ground state, except for the low lying states indicated.

Here we present the results of a preliminary survey of heavy metals which can be measured within three spectral regions in the UV which are accessible with existing CRLAS

technology (mirrors, detectors, and light sources). The results of this survey provide strong evidence for the capability of RSP to determine absolute concentrations for several metals simultaneously with a sensitivity which greatly exceeds detection limits of many other methods. Similarly, this discussion highlights the potential application to the identification of trace level molecular species. In Table 1., we list several heavy metals which can be monitored within three relatively narrow spectral regions.[11] Concentration detection limits are easily calculated by using the projected minimal detectable fractional absorption of the RSP apparatus, together with the path length and transition line strength.

The transition strength is commonly expressed in term of the oscillator strength f, which is a dimensionless number which scales linearly with the transition strength. The oscillator strength is easily converted to either the line strength S, or the transition cross section σ via inclusion of the lineshape function $g(\omega)$, which includes the effects of Doppler and pressure broadening, via:

$$\sigma(\omega)=S(\omega)g(\omega). \quad (4)$$

Concentration detection limits in the limit of weak absorption are then easily calculated by equating the minimum detectable absorbance (A_{min}) with the concentration (C) , path length (L), and absorption cross section (σ) via Beer's Law:

$$A_{min}= \sigma C L . \quad (5)$$

In the limit of weak absorption, the absorbance is essentially equal to the fractional absorption ($1-I/I_0$), since for $A<<1$, $e^{-A}=A$. For the sensitivity levels achieved in the Phase I apparatus (presented in Section 5), $A_{min.}=10^{-6}$, with an associated extrapolated limit in the UV of 4×10^{-6}. Using this value together with the above associated cross sections (via oscillator strengths) we can calculate the minimum detectable concentration for species in the table.

Take, for example, the specific case of mercury monitoring at atmospheric pressure. Current technologies have demonstrated a sensitivity of .2 mg/m^3 for mercury, which corresponds to ca. 6×10^{17} molecules/m^3. Techniques capable of achieving a detection limit of $<5\mu g/m^3$, or $<1.5 \times 10^{13}/m^3$ have recently been sought by the DoE. We can use the 253.65 nm transition together with Eq. 4 above after converting the oscillator strength into the cross section. In this case, $\sigma= 1.5 \times 10^{-14}$ cm^{-2}. This value is close to the experimentally determined value at

atmospheric pressure of 3.3×10^{-14} cm^{-2}, which is higher due to the blending of other isotopic spectral features. Using this value together with $A_{min}=4 \times 10^{-6}$, we arrive at a minimum detectable concentration for either free elemental Hg measured directly in the stream or a value for the total elemental concentration in the stream using an ICP source. In the first case, if we assume a absorption path length of 0.5 m, we arrive at a RSP detection limit of ca. 2.4×10^{7}/cc while with an ICP source with an effective plasma path length of 5 mm, we arrive at a detection limit of 2.4×10^{9}/cc. Both of these theoretical detection limits are in the part per trillion range, which greatly *exceed* existing EPA Methods (e.g. Method 101A).

The extension of the above analysis to other metals listed in the Table is straightforward and similarly indicates that for many metals *part per trillion detection limits for RSP will be routinely achievable*. For several of the above metals listed, the detection limits are significantly better than those given above for Hg (see associated *f*-values). From the above, it is clear that RSP should be capable of determining *absolute species concentration of multiple species simultaneously with extremely high sensitivity*. This capability will significantly advance the state of the art in chemical detection technologies, with the added benefit of being an all-optical method. In the Phase I Research Report below, we identify several other projected detection limits for high-priority heavy metals of immediate concern to the DoE. The potential for other applications within other Federal agencies such as the DoD is readily apparent in the above examples. Other applications potentially include the monitoring of radioactive elements, or chemical or biological warfare agents, as the RSP method is capable of providing ultra-trace level detection limits for molecular as well as atomic species. The general versatility and high sensitivity of the RSP technology further indicates the potential for a commercial or research-grade analytical instrument. Below, we present the results of specific market research performed for such development, following the discussion of integration of RSP for the aforementioned offgas analysis application.

Integration for Offgas Analysis

A primary concern in the proposed RSP development is the expected performance level of the technique under potentially harsh conditions of waste processing stacks. One of the primary MWFA concerns in this regard is the feasibility of the technology for use as a thermal waste treatment facility offgas monitor. In the past decade, we have performed several experiments using conventional CRLAS in environments ranging from flames to molecular beams, and have established to great extent the generality of the approach in environments similar to those of high or low temperature offgas streams.[12,13] We have similarly utilized the robust nature of CRLAS directly in flames[14,15] and laser vaporization plasmas of a variety of transition metals.[16,17,18]

RSP can be used as both a stack monitor to confirm emissions limits downstream of the process system or as a control monitor in the harsher conditions in the waste stream before the stack. In the first case, the conditions are relatively clean with temperatures in the 250-300F range and should pose no significant problem for in-situ applications. For the harsher elevated temperature (400-500 F) region before the stack, particle loading, high humidity, and corrosive and acid gases may exist. In this case, it may be necessary to employ strategies to keep the mirror surfaces free of particulates or corrosive chemicals, such as purging of the cavity mirror surfaces. Alternatively, sample extraction/heating preparation can be used, such as that currently employed for both FTIR and mass spectrometric detection methods. Possible configurations to achieve these goals are detailed in Fig. 3. Similar schemes may also be used in various other applications, such as the determination of iodine remediation efficacy in silver impregnated alumina filtration systems.[19] These examples constitute only a small fraction of the possible applications of RSP, which we believe is well suited for possible development of a general analytical instrument, as discussed below.

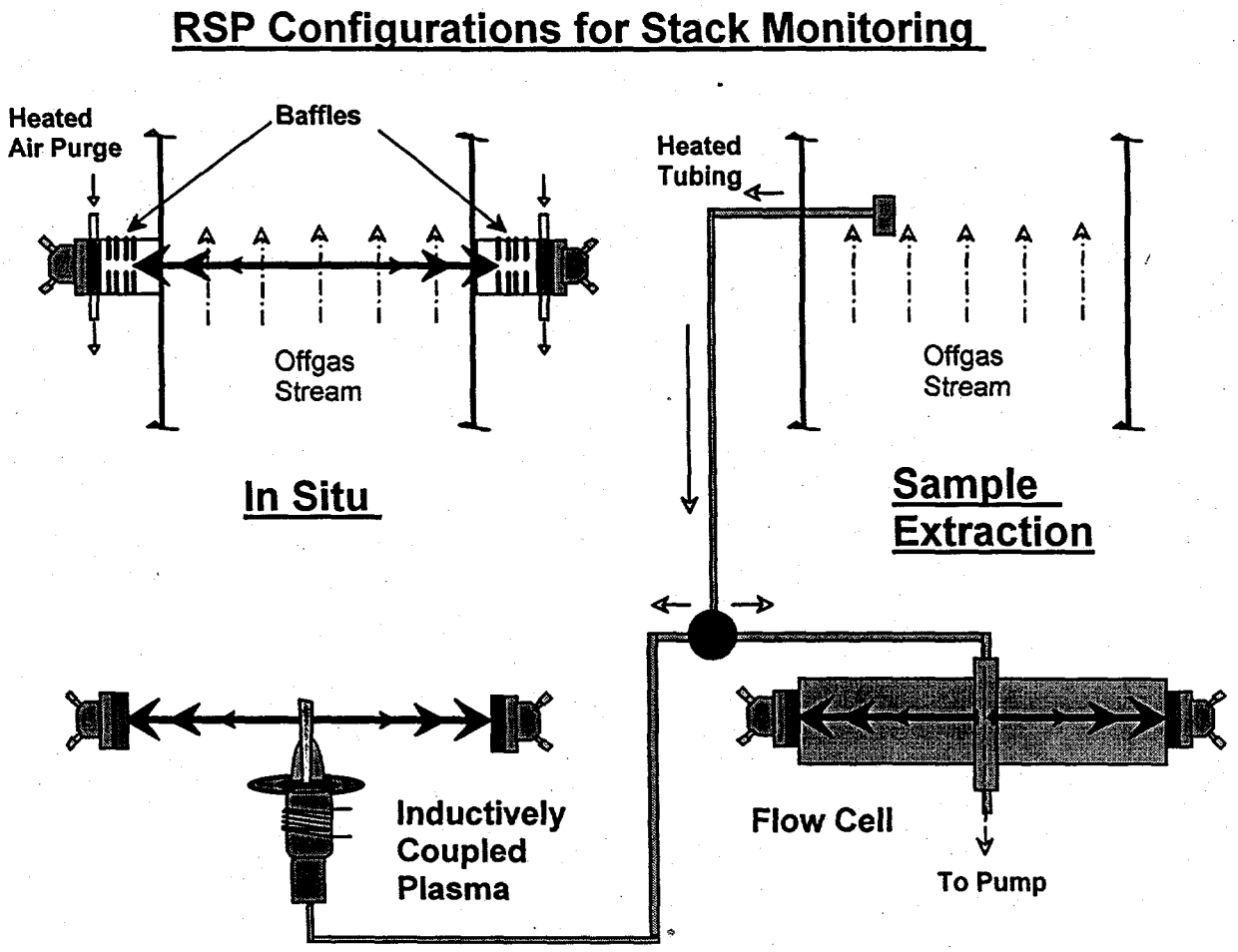

Figure 3. Integration of RSP with currently employed offgas sampling methods. When used in conjunction with an ICP atomization source, RSP will enable absolute elemental concentrations to be obtained on microsecond timescales. In cases where corrosive gases exist or soot particulates are formed, baffling and purging of the mirror surfaces can be implemented. Baffling alone has been effectively employed in laser vaporization plasma reactor studies as a means of protecting the coatings as well as keeping the highly reflective mirrors free of debris.

Commercial Potential and Significance of the Market

In this section, we explore the commercial potential for an analytical RSP instrument, by looking at the existing spectrophotometer market and projecting potential sales based on capturing a fraction of this market. The advantages of the RSP technique have been detailed above, and include high sensitivity combined with rapid data update intervals. We have contacted several commercial manufacturers of spectrophotometer and mass spectrometric

instruments, as preliminary research for the need for such unique capabilities. Specifically, we have contacted Perkin-Elmer, Nicolet, and Beckman. These companies specialize in the manufacture and sales of optical emission and absorption spectrometers, mass spectrometers, Fourier transform spectrometers, and other analytical instrumentation. Our discussions with personnel such as Dr. David Tracy, who is Vice President of Research and Development in the Analytical Instrumentation Division at Perkin-Elmer, indicate that the RSP technology we seek to develop will likely have real-world applications which are broad enough to warrant production of a commercial instrument. Of course, such development will in part be contingent on the ability to utilize less expensive light sources than that implemented for the Phase I and II research as presented here. With the recent development of a variety of solid state devices evidenced in recent years, we believe that candidates such as broadband OPO's currently exist in the visible and infrared regions, and over time will be further extended to smaller wavelengths. Some of these alternative light sources will be identified during the Phase II and III research. Nonetheless, the typically high price which accompanies instruments such as ICP-MS systems does not render the RSP technology as too expensive, even if pulsed laser systems similar in design to (but smaller than) those proposed for the Phase II effort are employed. Furthermore, the ability to achieve detection sensitivities equal to or better than such systems without the associated generation of secondary waste additionally suggests that the RSP technology will be competitive even if within the same price range as some existing instruments, which can cost in the $250,000 range.

In this section we briefly discuss the commercial market for the technology to be demonstrated in this proposed effort, as well as our plans for achieving this commercialization. To do this we organize the discussion into sections describing what the targeted market application is, the size of the targeted market, and our approach to developing the technology for commercial markets as well as our approach to reaching a commercial sales objective.

Market and Market Size:

The technology we propose to demonstrate and develop in this effort will be most valuable in making ultra-sensitive determinations of absolute concentrations of atomic as well as

molecular species, particularly metals, in the part-per-trillion concentration range. There are several commercial applications of interest for such an instrument. One such market, materials purity analysis for state-of-the-art semiconductor processing, often requires species detection limits of part-per-billion levels with absolute concentration assay. Techniques such as mass spectral analysis are typically used to test materials for the required ultra-high purity. While this technique has the necessary sensitivity, it is essentially impossible to quantify, except through elaborate controlled standard addition type of analysis. Extensive discussions with Dr. Cecilia Martner, head of the quality control analytical chemistry laboratory at Hyundai Electronics America (Santa Clara, CA), have convinced us that the capability we seek to develop is urgently needed to reduce wafer rejection rate and increase the quality of the most advanced devices. The instrumentation we propose to demonstrate can be used in an atomic absorption configuration to make absolute elemental concentration determinations of solid samples vaporized using laser ablation/desorption, or other atomization methods such as an ICP source.

Current instruments available for such analyses include the Optima 3300, a Perkin-Elmer instrument which combines EM with a bench-mounted ICP source. This instrument with peripherals and software sells for approximately $190,000/ unit, with total annual sales in the hundreds range. Another less expensive interment also offered by Perkin-Elmer appropriate for materials purity analysis is the SIMAA 6000 series atomic absorption (AA)spectrometer, which incorporates a graphite furnace. This system costs ca. $75,000, with annual sales again in the hundreds of units annually. Finally, the most sensitive instrumentation for these types of analyses offered by Perkin-Elmer is the Elan series 6000 ICP-MS system, which sells for approximately $250,000, again, with peripherals and software. This instrument has nationwide annual sales of approximately 100 units annually. It is relevant to note that the detection limits projected for the proposed RSP technology will meet or exceed the detection limits of these instruments in some cases by orders of magnitude (see Sections 5 and 7). If we estimate that the RSP technology can capture a 10% fraction of the above total market for these three instruments alone, annual sales in excess of $5,000,000 could be realized. If we estimate that an RSP instrument would cost in the above price range, and that only a few percent of the entire spectrophotometer/mass spectrometer market could be captured, the market size would be

significantly larger than this 5 million dollar figure. This significant market size, even for relatively expensive instrumentation, indicates promising commercial potential for RSP, if successfully developed.

Another potential market for the instrumentation we propose to develop is within the DoE itself, where the ability to detect trace levels of atomic species could be used to indicate the processing or storage of nuclear materials. This application is of importance to the DoE in verifying compliance with international nuclear processing agreements. Another potential DoE application is in the testing for releases of toxic or radioactive materials from power plants within the US, or similarly the monitoring of stored waste in sites such as Hanford. Again, the unique capability of RSP to optically discriminate between different isotopes of heavy metals (which in many cases is not possible with MS systems) without producing contaminated secondary waste is especially important. Below we analyze the market size for the development of an analytical instrument specifically for the semiconductor market, which indicates at the minimum level of the commercial potential of the RSP technology.

As mentioned above, the market size for analytical instrumentation for the specific application to semiconductors purity analysis is large and attractive. There are presently more than 40 semiconductor processing centers in the US today, as well as a smaller number of primary material suppliers. Each of these represents a potential buyer of the technology we seek to develop. Assuming that the price of an instrument could range from $100,000 to $300,000 (depending upon the sophistication of the unit), potential sales of 4 to 12 million dollars are possible within this market alone. As we develop the proposed technology we will be able to spread the development costs over a wider product base and produce more basic systems for lower cost, opening up wider markets in both scientific and commercial applications.

Approach:

The approach we will take in developing a viable commercial market for the technology we propose to develop is based upon an approach we have recently successfully taken to commercialize another technology we have developed. Specifically, we have actively developed

and marketed CRLAS relevant technologies, including ultra high reflectivity mirrors and other optical components for these systems. This specific commercialization has resulted from our close collaborative efforts with thin-film technology vendors, together with our development of suitable diagnostics (via SBIR research) for assessing the quality and performance of the associated optical components (mirrors primarily). This effort has resulted in sales exceeding $60,000 in the last 9 months, which represents our initial foray into marketing specific products. We project market sales well over $100,000 in the next year on just a few of the peripheral technologies which we have developed as a result of previous Phase I SBIR/STTR contracts. In the present case, our corporate approach to the development of sophisticated analytical instrumentation is to combine our strengths with those of industrial partners to reach commercial customers as rapidly as possible. In this case, we will license our technology to interested companies, and work closely with them to achieve rapid product development, which would otherwise prove difficult for a company with our relatively modest facilities. We are currently discussing this possibility with Perkin-Elmer, who has successfully marketed analytical instrumentation for decades. By collaborating with an established commercial instrument vendor, we exploit the capabilities of a strong and established marketing force as well as name recognition in a particular market. We have discussed such collaborations with Dr. Fumitomo Hide of Raychem, as well as David Tracy at Perkin-Elmer for the technology discussed here, and are presently assessing the commercial potential of the RSP technology for instrumentation development. Similarly, we have established research ties with other groups working on DoE funded research to integrate the RSP technology into existing missions within the Federal government, including groups at Sandia national Laboratories Livermore (Dr. Tom Kulp), and Mississippi State University (Drs. Winstead and Miller) We plan to pursue commercialization of the present proposed SBIR along similar lines, identifying likely markets while establishing realistic product specifications and prices in the process. As the RSP technology is still in the development phase, it is not currently possible to assess these values accurately at this point in time. However, as demonstrated in the following section, we believe the Phase I research indicates exciting possibilities in the commercial sector for an RSP-based analytical instrument, as well as a variety of Missions within the Federal Government.

5. Accomplishment of Phase I Objectives:

PHASE I RESEARCH REPORT:

In this section, we present the results and conclusions of our Phase I research, and detail to what extent the Phase I objectives have been met. This section also constitutes the Phase I Research Final Report, and describes in detail the specific Tasks performed to date on the development of RSP. From the data obtained during the Phase I effort, we are able to extrapolate to obtain the operable regimes for the proposed Phase II RSP instrument. Some of these extrapolations are briefly mentioned in this section, and in explicit detail in the Phase II Work Plan (Section 7). Before presenting a detailed description of the Phase I research, we briefly review the Phase I Research Objectives below. The experimental data presented in this section demonstrates achievement of and beyond these Objectives, including the first successful construction of an integrated "streak camera"/ frequency dispersing RSP instrument, which was initially slated for the Phase II effort.

Summary of Phase I Objectives:

Objective 1. Demonstrate the feasibility of the rotating mirror/CCD "streak camera" principle for recording the ringdown (decay) time of the cavity. Determine the specifications required of the associated components.

Objective 2. Develop data acquisition, handling, and equipment-to-computer interfaces for automated scanning.

Objective 3. *Design* the frequency dispersing optical assembly at cavity output incorporating the streak camera concept, and verify specifications required of associated components.

Objective 4. Determine requirements and constraints on visible/UV broadband light source for use as RSP injection laser.

Objective 5. Determine experimentally achievable RSP sensitivity and spectral resolution based on results of above Objectives.

Objective 6. Calculate expected performance levels for the monitoring of specific DoE target species (number and minimum concentration) based on sensitivity levels dictated in Objective 5.

Description of Tasks Performed in Phase I and Associated Milestones

Tasks 1 and 2. *Demonstrate the streak camera principle and establishing a triggering scheme for synchronizing the mirror with the pulsed laser and data acquisition:*

The first two Tasks performed in the Phase I research comprised of demonstration of the streak camera principle (Task 1), including establishing an adequate triggering scheme for the firing of the laser and the gating of the detection electronics (Task 2). Special emphasis was placed in these Tasks on establishing routine performance levels for a relatively simple experimental configuration of modest components. This emphasis allowed the feasibility of using off-the-shelf, lower-cost (i.e. not research grade) extracavity hardware to be assessed. This hardware included a standard (uncooled) Pulnix TM7AS 1/2" format CCD array ($800) and a Mu-Tech IV-450-4M framegrabber ($800). The use of a cooled CCD camera would allow roughly two orders of magnitude less light to be used than that of the present initial study, at an additional cost of ca.$10K-20K. All of the work described in this section was performed at Los Gatos Research by Drs. Scherer and O'Keefe, using equipment supplied entirely by LGR at no direct cost to the Phase I effort.

The experimental apparatus constructed for Phase I is depicted in Fig. 4 on the following page. The cavity input light was produced in a Nd:YAG pumped dye laser system (Lumonics 532 nm and Continuum ND60 dye laser, respectively) and sent into a simple Newtonian telescope which incorporated a spatial filter between the two positive lenses. The beam was reduced in this arrangement to be approximately 1 mm in diameter (at the cavity input mirror) with minimum divergence and good TEM00 mode quality. A click-in mirror was used to directly measure the injection laser energy (per pulse) at the input side of the cavity at will. The cavities employed for Phase I were either open-air cavities or vacuum cell cavities, wherein the mirrors also served as cell windows. The light was injected on-axis into the ringdown cavity, reflected off of the rotating mirror, and onto the CCD detector. The CCD was a standard 1/2" format array with 760x490 pixels, each pixel measuring 8x9 microns. The data were collected across 640x480 of these pixels, using the RS-170 output of the camera, and digitized in the

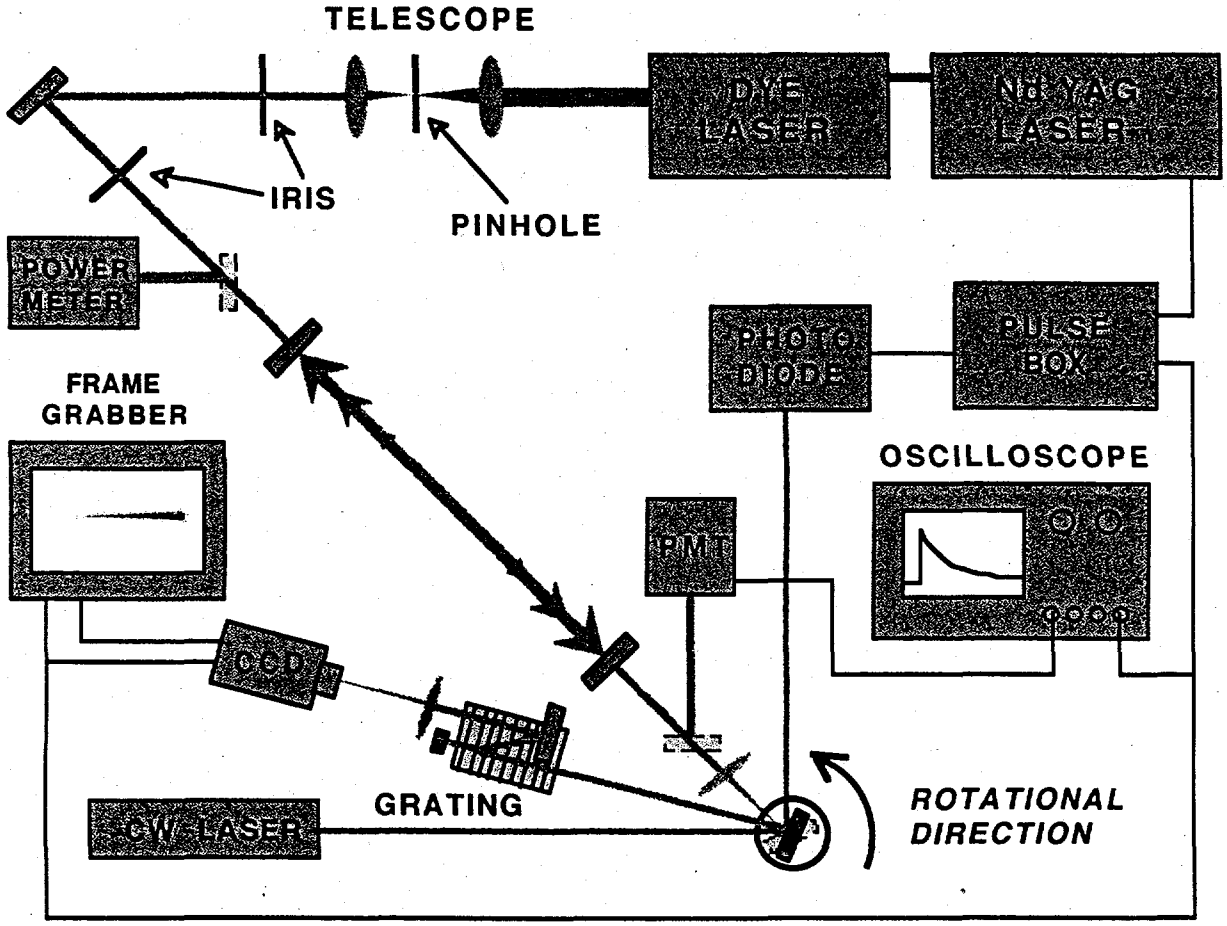

Figure 4. RSP experimental apparatus: Timing of the experiment is achieved by reflecting a cw laser off of the rotating mirror and onto a photodiode. The first Tasks were performed without the diffraction grating present.

framegrabber with an 8-bit A:D converter. The camera was used in the asynchronous mode with an internal shutter speed of 1/31,000 s (ca. 32 us), which significantly reduced background signal. A click-in mirror was also employed in between the cavity and the rotating mirror, in order to monitor at will the decay event with the standard PMT /digitizer (Tektronix TDS 360 digital storage oscilloscope) method used in pulsed CRLAS. This configuration allowed for comparison and calibration of the streak camera measurements.

Various focusing schemes were explored to image the streak trace at the CCD array, in order to adjust the spot size and associated signal fluence. This allowed issues related to the dynamic range and sensitivity to be addressed, such as achieving adequate A:D dynamic range while maintaining adequate time resolution (spot size vs. total # of pixels). The cavity was initially aligned using the standard procedure of retroreflecting the input beam through one or more irises located on the input side of the cavity. It was found that use of the CCD detector (with a stationary mirror) facilitated fine tuning of the cavity, as the spatial "walking" of the beam could be directly monitored and minimized. Similarly, the CCD also served as an excellent diagnostic of the injection light transverse mode quality.

For these Phase I experiments, a continuously variable speed ac-motor was employed to drive the rotating mirror at the cavity output, in order to translate the time dimension of the cavity decay event into the spatial dimension of the CCD camera. This motor was chosen for several reasons, the primary reason of which was that an essentially infinite range of speeds (from 2000 to 15000 rpm) could be achieved. This allowed various geometric configurations to be explored while adjusting the rotational speed and delay time (between the firing of the laser and the mirror position) to ensure a good "fill-factor" of the decay event at the CCD array. Research-grade, air-bearing optical spindles assemblies, which would have been the other alternative, come preset for only a few rotational rates (due to balancing requirements), which for these Phase I studies would have significantly limited the flexibility of the extracavity optical geometries. Additionally, we wanted to explore the feasibility of employing inexpensive alternatives to the typical $5000 cost of an air bearing assembly. For these reasons, we employed a simple ac, brush contact, double bearing construction motor and induction-type speed control, the sum of which cost less than

$150. Somewhat surprisingly, these components proved more than adequate for the single shot "streak camera" measurements presented below. In the event that signal averaging is desired (as will be explored during Phase II), an optical spindle assembly would be more desirable, as the rotational stability is significantly better than that of the brush-type motor used. Using a series of fast photodiodes and detectors, we determined the per cycle rotational stability of our brush motor to be better than 1 us/30 degrees of arc while the long-term rotational drift of the motor was much more significant (10-100 us/sec). As the single shot streak traces presented below required only a few degrees of arc to fill the CCD frame, the resultant maximum nonlinearity of the streak trace data obtained was < 100 ns/50 us, or less than approximately 0.2%. As shown later, this degree of precision introduces a negligible error to the streak trace measurements.

A first surface reflector of ca. 1/2" square was secured directly to the beveled motor shaft and aligned such that the ringdown axis was perpendicular and coincident with the mirror rotational axis at normal incidence. As the rotational speeds required of the mirror resultant in frequencies which are higher than the 20 Hz maximum repetition rate of the laser system, a scheme was devised to synchronously trigger the laser at harmonics of the mirror rotational speed. This scheme was inherently insensitive to the long-term instability the inexpensive brush motor optical spindle assembly, and could similarly be employed for low-cost commercial devices.

Triggering of the cavity injection laser, CCD, and framegrabber with respect to the rotating mirror was initially achieved by reflecting a cw HeNe laser off of the rotating mirror and onto a photodiode, as diagrammed in Fig. 4. The photodiode was then used to trigger a standard pulse generator (Stanford Research DG535), which subsequently triggered the firing of the flashlamps and Q-switch of the Nd:YAG laser. The CCD camera and the framegrabber (and digital oscilloscope for CRLAS measurements) were triggered at the same time as the firing of the dye laser. The delay between the firing of the flashlamps and the photodiode signal was adjusted (with the delay between the Q-switch and the flashlamps kept constant) to time the placement of the cavity decay light precisely onto the CCD array. The mismatch between the rotational frequencies of the mirror and laser system was addressed by adding a 50 ms delay on

another channel of the pulse box to the Q-switch delay time, resulting in a trigger "rate error". This effectively kept the pulse box from responding to the next several external trigger pulses from the photodiode. After the 50 ms delay, the pulse box was again ready to receive the external trigger signal from the photodiode in a synchronized fashion with the rotating mirror. In this fashion, the mirror rotational speed could be adjusted to any arbitrary speed (down to 20 Hz) without effecting the firing rate of the laser system. For RSP systems in future configurations which employ "on-camera" averaging, an encoder wheel on the motor shaft, or a constant velocity system could replace the timing box scheme as presented above. Nonetheless, the method employed proved extremely effective as well as versatile. An iris and a color filter were placed in between the photodiode and the rotating mirror to minimize the response of the photodiode to stray (primarily Nd:YAG) light. The HeNe laser used for the trigger light source was later replaced with an inexpensive blue, air-cooled Ar-ion laser. This was done to explore the use of bandpass filters at the CCD to minimize background scatter of the trigger laser, which was at the same wavelength as these initial 630nm RSP experiments.

The proof-of-principle streak camera data were recorded in the 620-645 nm region with single pulses of injection laser light consisting of tens of microjoules per laser pulse. All of the streak camera data presented here is single-shot data, with decay times ranging from 5 to 15 microseconds. The initial measurements were recorded with either one or two focusing elements placed in between the cavity and the CCD, with good camera dynamic range achieved with a single element placed in between the cavity and the rotating mirror. As shown below, the ability to saturate the pixels with modest focusing of the cavity output indicates that smaller spot sizes could be combined with significantly less laser light while still achieving good dynamic range. The first series of streak traces obtained were acquired without the frequency dispersing grating assembly as shown in Fig. 4.

A typical streak trace for a well aligned cavity is shown in Fig. 5, which displays the exponentially decaying signal over the horizontal axis of the array for only a small vertical portion of the array. The data are displayed as a light trace against a dark background and include ca. 30 microseconds of the decay event.

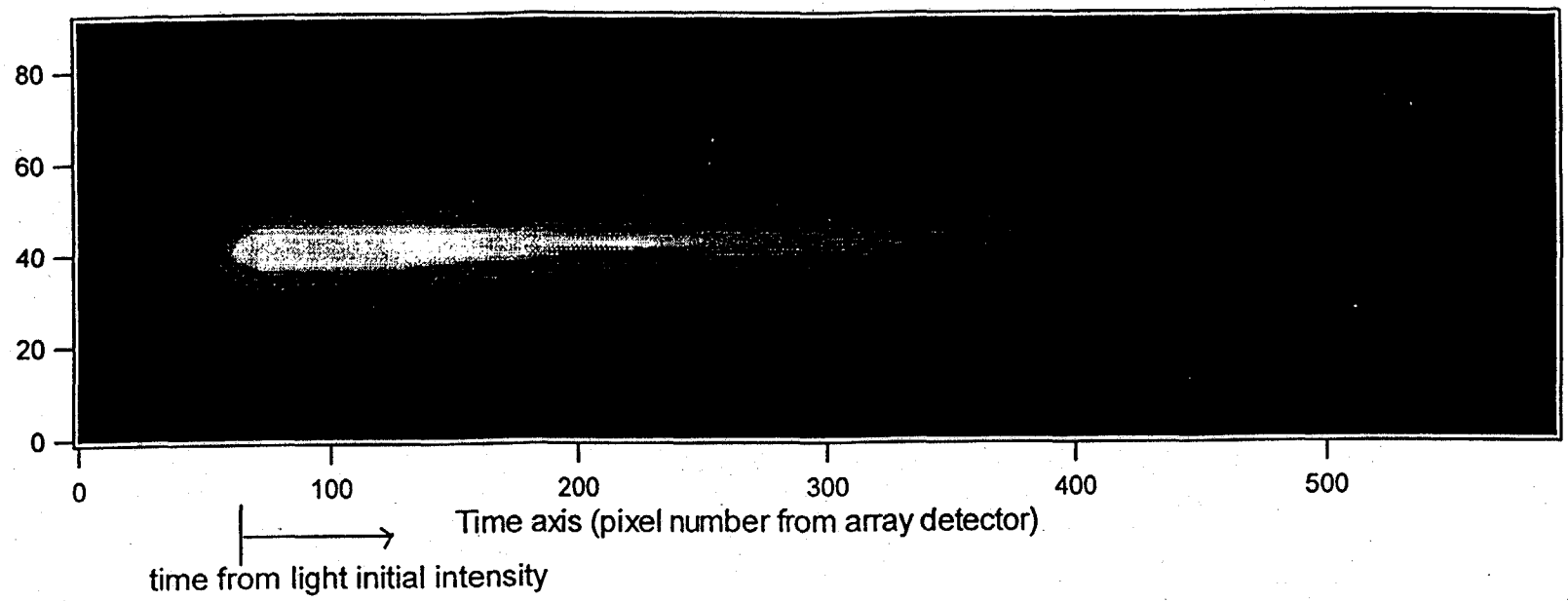

Figure 5. RSP single shot streak trace obtained with a mirror rotational speed of 7100 rpm, and an injection laser fluence of 100 uJ/pulse, as measured before the input mirror. By integrating across the streak, the corresponding photon lifetime inside the cavity can be determined. In this frame, ca. 30 microseconds are displayed.

In this scan, the mirror rotational period is 8.4 ms (7100 rpm), the cavity length is 32 cm, and the corresponding cavity losses per pass (as measured with CRLAS) are 100 ppm. This single-shot measurement was obtained with an open-air cavity at 632 nm with a total energy at the (outside of the) cavity input mirror of only 100uJ. A single focusing element was positioned between the cavity and the rotating mirror (close to the rotating mirror), and the camera was positioned near the focal point of the lens, which was approximately 30 cm. In this configuration, the timescale of the ringdown event is translated into the horizontal axis of the array with a corresponding time base of ca. 40 ns per pixel. As shown in Fig. 5, the vertical dimension of the spot at the CCD with this arrangement is such that the FWHM is approximately 20 pixels wide, or 160 um, which is far from the diffraction limit for this frequency. This spot size was adjusted to prevent damage to the CCD, and can, as shown later, be further reduced with less light. These data were obtained running the dye laser near threshold, and thus do not represent the achievable brightness for the laser system employed. The streak traces obtained as shown above were then analyzed to yield corresponding optical cavity losses in the manner described below.

These RSP "streak camera" data were compared with CRLAS measurements obtained by swinging the folding mirror into the optical path at the cavity output mirror and directing the signal onto a standard photomultiplier (Hammamatsu R912). This configuration allowed the RSP data to be calibrated as well as checked for linearity. Losses for the same set of mirrors were measured for several different cavity sizes, and yielded the same reflectivity values from the differing decay times. The linearity of the system was also verified on measurements on absorbing samples, as presented later. In addition to facilitating calibration of the streak camera data, the comparison of the two measurements led to a variety of interesting observations, which are primarily apparent only in the streak camera data. In particular, the RSP measurements enabled the time evolution of the cavity transverse mode structure to be recorded as a function of cavity alignment, while the overall effect on the decay time was monitored.

In Fig. 6, three independent streak measurements are displayed for decreasing degrees of cavity alignment. These data are inverted (black on white) and the background count is

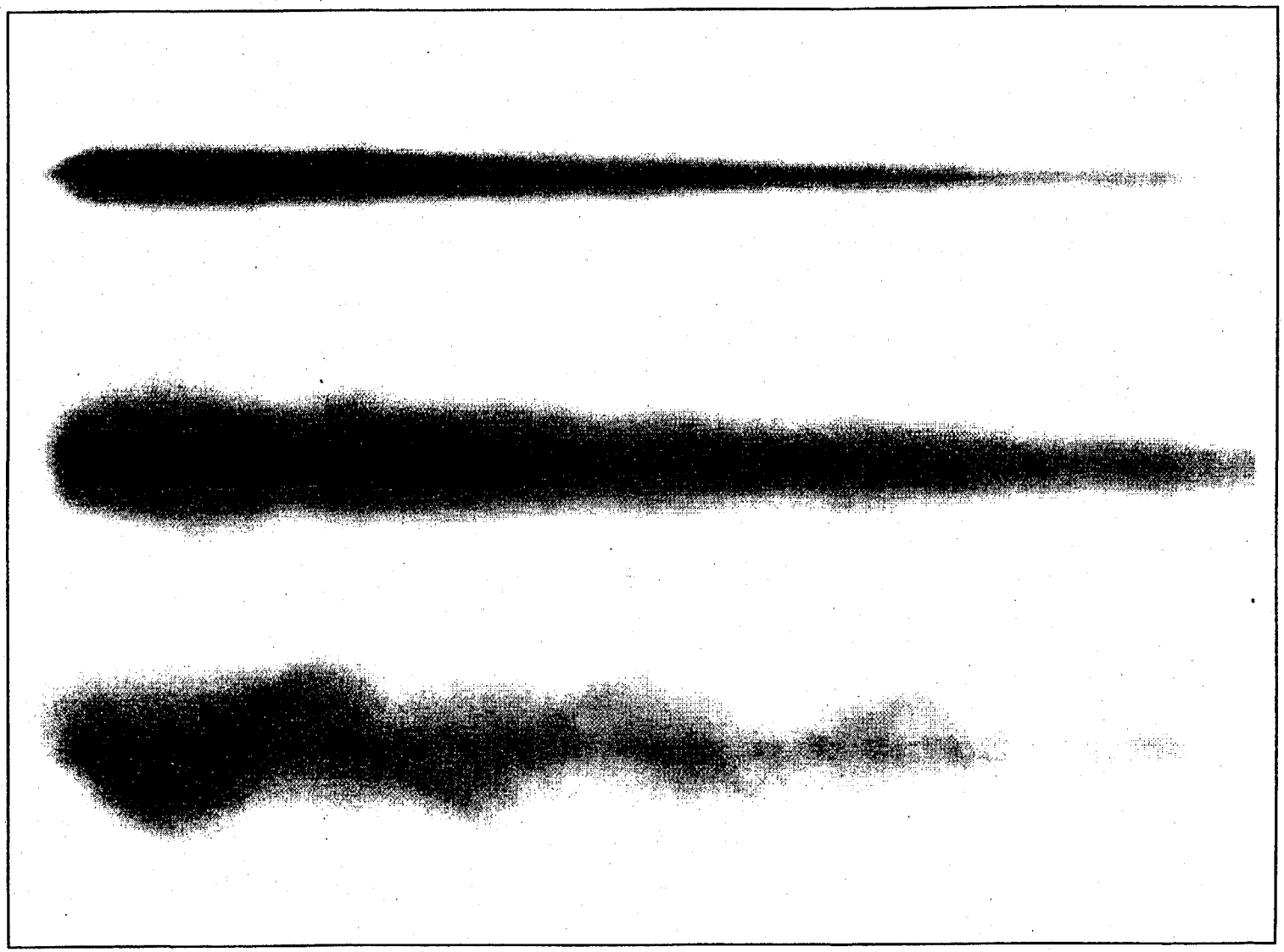

Figure 6. RSP traces obtained for three degrees of cavity alignment. The cavity was intentionally misaligned for the lower two traces, which exhibit significant walking of the beam as the light multipasses the cavity.

subtracted to highlight features of interest. These data are not normalized for differences in laser fluence. In the top streak, the cavity alignment is optimized for maximum decay time and streak trace length, and the resultant decay displays axially symmetric features. In the middle trace, which is expanded horizontally (in time), the cavity is slightly misaligned, resulting in the appearance of asymmetric and periodic features. In this trace, the corresponding decay time is virtually unchanged from that of the upper trace, in spite of the irregular features observed in the trace. This type of phenomena can lead to anomalous decay times when detectors are used with elements which are smaller than the output spot, or when limiting apertures are placed in between the cavity and the detector. Similarly, in the streak trace measurements, the entire signal must be integrated (in the horizontal axis in this case) to extract accurate decay times. In the lower trace (also expanded horizontally), the cavity is further misaligned, and a spiral pattern results from the off-axis beam "walking" of the light as it multipasses the cavity. In this case, the cavity decay time is significantly degraded. In these examples, the ability of RSP to obtain detailed information about the cavity alignment or stability can be used in a complementary fashion to maximize the performance of the instrument for spatial resolution within the probe region of the cell or source. Fluctuations in, for example, a discharge plasma, will be observable on a microsecond timescale, as different regions of the decay can be selectively fitted. These data graphically display the unique ability of RSP to be used simultaneously as a diagnostic of the cavity alignment quality, as well as to assess the degree of spatial mode matching achieved.

The surface intensity plot for the data shown in Fig 6 is graphically displayed in Fig. 7, which shows that a significant portion of the initial decay for the middle and upper traces is saturated at its maximum 8-bit value. In this case, only the unsaturated data should be used for fitting of the decay times. Similarly, if the decay event is short compared to the spatial extent of the pulse, it may not be possible to extract the decay times. In the present data, the spot size is only a few percent of the total streak trace, which does not impede the ability to accurately determine the cavity decay times. This point will place a limit on the dynamic range achievable with a RSP apparatus. As the streak traces are reduced to 2-3 pixels, the dynamic range will equal that of conventional CRLAS, which is typically three orders of magnitude. The data in Fig. 7 are translated into decay times by first integrating the streak trace in the vertical dimension, and

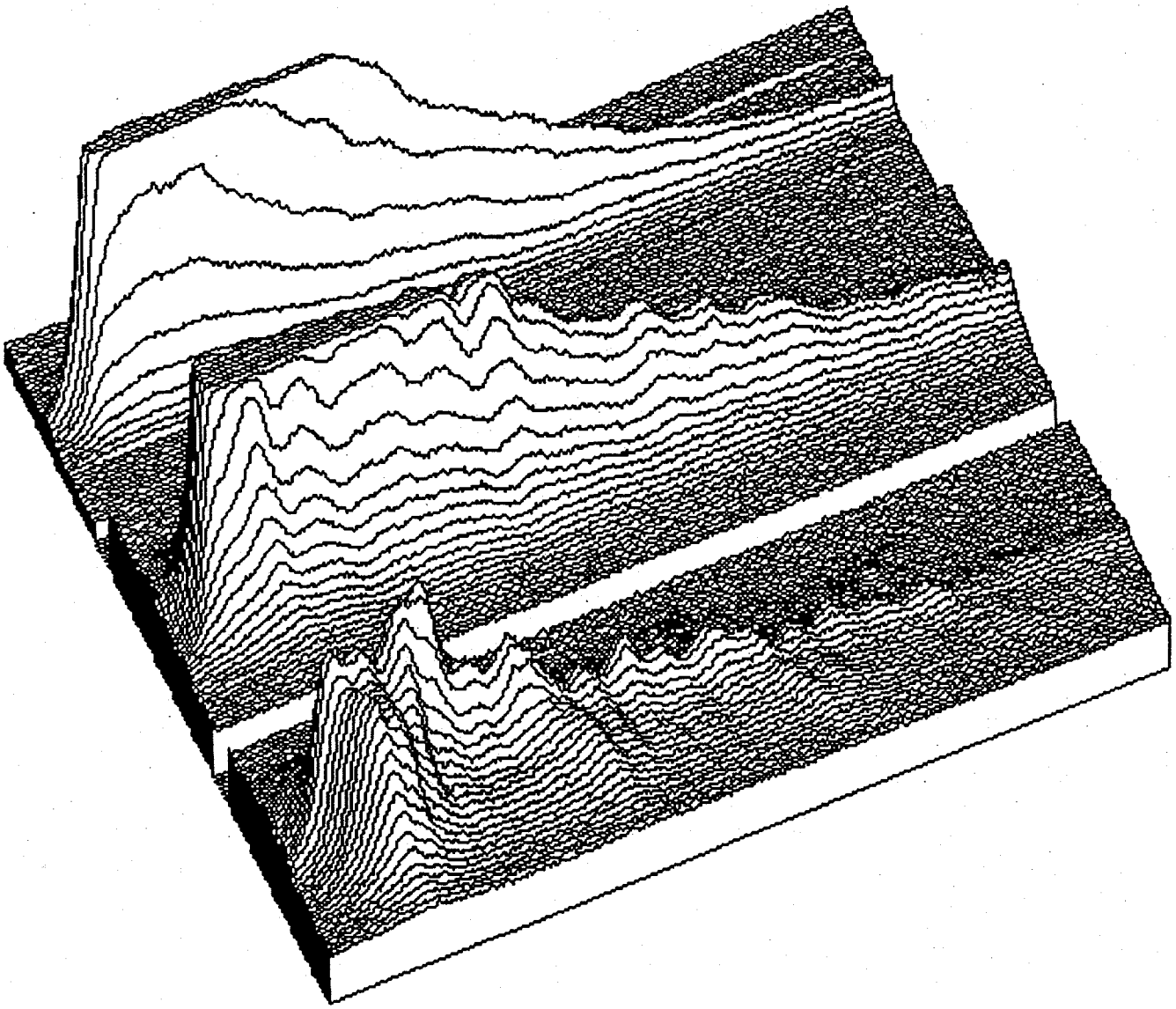

Figure 7. Surface plot displaying intensity levels for the streak traces presented in Fig. 6. Saturation of the pixels in the early part of the decay is evident in the upper two traces, while the lower trace exhibits significant spatial modulation across the CCD detector.

fitting the subsequent decay profile in the unsaturated region. The time base is easily established by using the CRLAS measurement to calibrate the RSP signal. Alternatively, the geometric configuration of the assembly could be used together with the mirror rotational speed. For a commercial instrument, calibration would be performed using the CRLAS method across the frequency range of interest.

In Fig. 8 on the following page, the integrated streak trace profile is shown for the top trace in Fig. 7, together with the CRLAS measurement and a single pixel wide row of data taken through the central region of the same streak. This comparison of the single pixel data identifies the unsaturated region of the integrated profile, which can be reliably used for fitting of the decay. A striking feature of this comparison is the relative noise levels between the RSP data and the CRLAS data. In this case, the noise level for the RSP data is significantly lower than that observed in the CRLAS data. This difference is manifest as a smaller uncertainty in the associated fitted decay times, which are also shown for both sets of data in Fig 8. The standard deviation of the fitted decay time constants in this case were found to be 0.7% and 7% for the RSP and CRLAS measurements, respectively. For the mirrors used in these experiments (R=99.99%), this translates into per pass fractional absorption sensitivities of $7x10^{-7}$ and $7x10^{-6}$ for the RSP and CRLAS data, respectively. The lower sensitivity of the CRLAS measurement in this case in part results from the relatively high rf noise from the Nd:YAG laser and motor assembly which is subsequently picked up by the fast phototube electronics. This comparison highlights that RSP can be implemented in electrically noisy environments, as the CCD array is largely insensitive to rf noise, such as may be encountered in discharge or plasma sources. The 0.7% standard deviation obtained with the RSP measurement is similar to the 1% values commonly reported in CRLAS measurements which employ signal averaging. The increased sensitivity in the RSP-obtained cavity decay data in part also results from the larger effective number of "detectors" employed in the array, which of course will be of decreased benefit as fewer pixels are illuminated. Nonetheless, these data demonstrate that the RSP method should be capable of achieving sensitivity levels comparable to or better than those demonstrated for CRLAS even at the 1-2 (vertical) pixel illumination regime. This point also has direct consequences for the achievement of wavelength resolution in the frequency-dispersed apparatus.

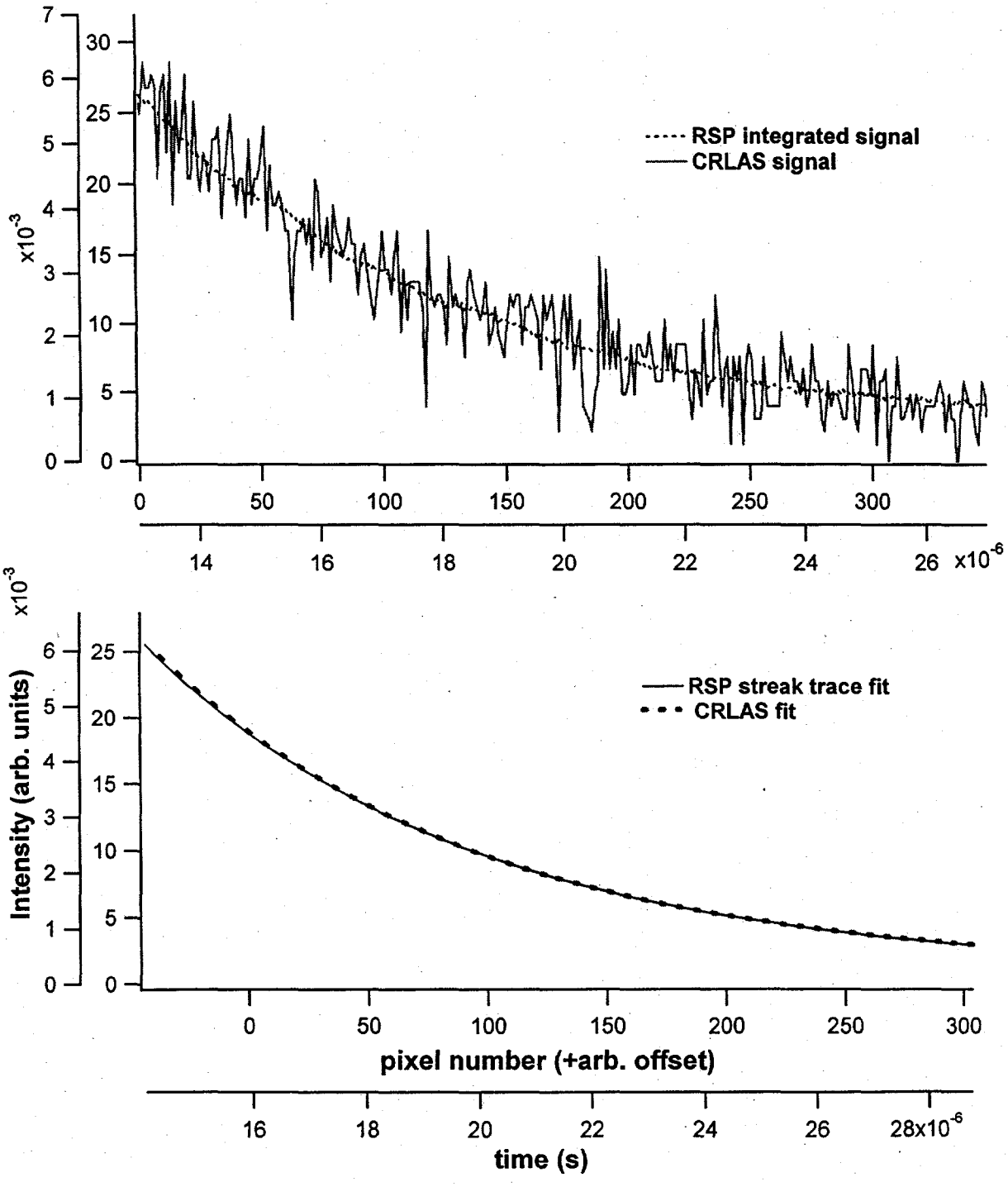

Figure 8. Single-shot RSP vs. CRLAS data (top) and associated exponential fits (bottom). The reduced noise in the RSP data results in an order of magnitude smaller standard deviation of the extracted decay time constant. These direct comparisons alsoallow the RSP data to be calibrated, effectively establishing a relationship between pixel number and time.

Similar measurements and data analyses were also performed with different length cavities, different camera to mirror distances, and different spot sizes. In all of these measurements, the ability to obtain accurate decay times with RSP was confirmed. This relationship is explicitly demonstrated later in this report for the case of an absorber placed in the cavity. With the double-bearing motor used in the above experiments, the wobble was almost immeasurable up to the 0.5 m mirror to camera distances employed. This indicates that relatively inexpensive spindle assemblies could be used for a low cost instrument, together with the obvious extrapolation to more sophisticated air-bearing spindle assemblies.

Milestones of Tasks 1 and 2:

These experiments established that the "streak camera" principle can be successfully implemented for recording the cavity decay time. These Tasks also unexpectedly demonstrated that the RSP method can exceed the performance levels of conventional CRLAS, especially in electrically noisy environments, using low cost, off-the shelf components. The streak camera method was also found to be an excellent means of characterizing the alignment quality of the cavity, as well as the time evolution of the mode excitation of the cavity.

Task 3: *Develop software for data acquisition and handling:*

During Task 3, we developed the framework for automated data acquisition and processing, and began the initial development of software interfaces and subroutines for the control of individual components. We used a Labview-based program structure for the overall design, with a GPIB interface for the oscilloscope data transfer (for CRLAS measurements), and a commercial framegrabber board which is housed within the computer for recording and saving the 2-D images in either TIFF or Bitmap (BMP) formats. In these initial Phase I studies, a narrowband tunable dye laser system was employed, and was used in a stand-alone format with its own software, as the overall RSP design will employ a different light source, which in most applied configurations will not require any tuning or programming software whatsoever. For a commercial or stand-alone instrument for in-situ monitoring, a stripped-down program will be developed which will include a operator-friendly environment for data acquisition and

processing. In this case, the software will be tailored to display species concentrations directly, including identifying potential interferences, etc.

The data processing and analysis in these Phase I studies was performed manually in a single streak fashion with a combination of commercially available math programs (such as IGOR and Excel), and image manipulation software such as NIH image. Standard, least-squared fitting routines were employed for fitting the decay times, and included background subtraction as well as checking for multi-exponential character (by fitting adjacent regions of the decay). This manual handling of the data was essential in Phase I in order to qualitatively and quantitatively address a variety of issues including pixel saturation, dynamic range, background subtraction, reproducibility, and spatial specificity. For example, in Tasks 1 and 2, we demonstrated how to properly fit the streak trace data by integrating the signal over the spot size of the cavity output, and fitting only regions where no saturation occurs. As a result, the programs for the Phase II broadband RSP instrument will include variable pixel grouping fitting routines, which will effectively incorporate the experimentally achieved frequency (spatial) resolution. This will be required in the broadband instrument, since a continuos image will be produced, instead of discrete streak traces as shown here.

The program which we will develop during Phase II will be designed to be used in a plug-in fashion with the existing Phase I Labview-based program structure, and will include image acquisition routines for seamless file transfer from the framegrabber to the main program. The data transfer rates from the CCD to the computer were routinely in the Ms/sec region, translating into 3-4 full frames of data per second for the board used. Frame grabbers with ten times this data transfer rate are also available, however, this data transfer rate is more than adequate for the data update interval of < 1s sought by the DoE for real-time species monitoring. The subtleties associated with the fitting routines mentioned above are made more apparent in the following discussion wherein we describe the Phase I construction of a frequency resolved RSP apparatus.

Milestone of Task 3:

The structure required for the fully integrated RSP program was developed, and the associated subtleties in data handling to be addressed during the Phase II effort were identified. The Labview-based program structure employed in Phase I was utilized for its simplicity, user-friendliness, and expandability. The data transfer rates attainable with of-the-shelf framegrabbers was found to be adequate for the data update intervals of < 1s.

Task 4: *Design wavelength separation extracavity optics for the Phase II apparatus:*

Initially, Task 3 of the Phase I effort was geared to accomplish design of the frequency dispersing optical assembly, for subsequent construction in a Phase II apparatus. Instead of confining these efforts to theoretical designs, we decided to additionally construct an extracavity dispersing assembly, which would establish a knowledge base from which to extrapolate performance levels for more sophisticated designs. In this section, we present the data from the first functioning RSP apparatus, which employed the narrowband laser system in a proof-of principle demonstration. In this case, the laser light was tuned with the grating in place, resulting in a spatial displacement of the streak trace along the other (orthogonal) dimension of the CCD. These results indicate that extracavity dispersion of the cavity light can be combined simultaneously with the streak camera approach to produce a two-dimensional image of frequency vs. time, and hence frequency vs. absorption. These RSP data were then quantified as discussed previously to obtain the frequency-dependent losses of an optical cavity with an absorber present, across a broad region of the visible spectrum.

The design criteria for the extracavity optical assembly were based on well known fundamental optical principles of dispersion. For example, the theoretical grating resolving power (R) is determined by the product of the grating order (m) and the number of lines (N) illuminated (R=mxN), which is determined by knowing the line density and the spot size on the grating. In a monochromator, which is essentially what the RSP extracavity optics comprise, the experimental resolution achieved is dictated by the product of the slit width and the reciprocal linear dispersion, and will be further degraded by aberrations of the optical system. In either case, the dispersion achieved can be increased by illuminating a greater number of lines as well as increasing the order. For our Phase I research, we chose to work with a modest dispersion

which would allow adequate deflection at the CCD for proof-of principle studies. Thus a grating with 1200 lines/mm was used while illuminating < 1 cm of the grating, to achieve an effective scanning bandwidth at the CCD of ca. 20 nm in the 630 nm region. Further dispersion would be easily achieved by simply expanding the beam along one axis of the grating and subsequently refocusing the light into the CCD. For these initial experiments, we did not explore the achievable dispersion limit of the system, but below, following presentation of the first RSP results, we present the design specifications for the theoretical as well as achievable dispersion of the Phase II apparatus, which was designed for UV operation.

The experimental configuration employed for these initial RSP demonstrations was as previously shown in Fig 4, which is essentially a top view of the apparatus. In these studies, a grating with 1200 lines/mm was oriented at approximately 60 degrees (with respect to the vertical axis), and the cavity output illuminated approximately **7 mm** of the grating. The zero order reflection was absorbed by a beam block and the first order of the grating was retroreflected in an upward fashion to a first surface optic. The light was then reflected in a forward fashion to be parallel with the light from the rotating mirror, while displaced vertically ca. 5 cm. The diffracted light was then focused into the CCD array with a 2" spherical lens with a 160 mm focal length located close to the grating. Careful alignment of the components (the grating especially) was performed to assure that the streak traces were parallel to the horizontal axis of the array. The laser was then scanned in frequency and the subsequent streak traces were recorded as they were displaced along the (vertical) axis of the array. The components were adjusted to achieve an effective displacement across the entire vertical axis array over a tuning range of ca. 20 nm (625-645). Using this simple arrangement (with the grating used only in first order) with streak width of approximately 7 pixels, the effective resolving power of the instrument for this tuning range was measured to be ca. 2000, or 0.3 nm. This effective resolution was limited by the number of pixels illuminated at the array per streak (slit width), while the actual design resolution was closer to 8,000. It was found that the resolving power measured as displacement of the streak at the camera) could be doubled by simply picking off the second order, which was considerably weaker. The 20 nm design goal in these initial studies was chosen to facilitate the measurement of the overtone spectrum of propane, which was introduced

into the cavity to demonstrate the RSP method. Again, the results of these experiments serve as a proof of principle of the RSP method, and do not represent the dispersion limits of the apparatus in this wavelength region.

In Fig. 9, the overtone absorption spectrum of propane is shown as measured by both the RSP method as well as CRLAS. The fitted decay times for the RSP data are shown at 1 nm increments, and were performed as discussed previously. Again, saturated regions in the early part of the decay are omitted from the fit in, for example, the 640 nm trace. The dimensions of the individual streak traces represent the actual displacement measured at the CCD as the laser was scanned in frequency in a pointwise fashion, although the image itself is manually constructed from 21 individual full-frame files. The CRLAS measurements also shown in Fig. 9 were obtained by signal averaging 8 laser shots per wavelength point, at a step size much smaller than that used for the RSP measurements. The standard deviation of the fitted decay times for the RSP data again ranged from 0.5-1%, with associated per pass absorption sensitivities of ca. 1 ppm. Here the effective wavelength coverage of the apparatus is over 20 nm, while the spatial extent of the individual streaks limits the effective resolution to approximately 1/3 nm. Again, the traces are single-shot measurements, with an average energy of 40 microjoules per pulse.

The most striking feature of the RSP data is the ability to almost "see" the resulting absorption spectrum in the relative lengths of the individual streak traces. Additionally, the fitted streak trace data demonstrate that the RSP method is essentially unaffected by large variations in the absolute intensity of the light across a given bandwidth, as is the case in conventional CRLAS. For example, the streak at 625 nm is nearly four times weaker than that recorded at 645 nm, yet accurate absorption intensities are nonetheless extracted. These data demonstrate conclusively that RSP can provide quantitative absorption data across a relatively broad spectral region with high sensitivity. Extension of the proof of principle demonstration presented here to include broadband light sources will be explored in Phase II, and is a straightforward extension of the above configuration. The results presented here using a simple dispersing configuration can be extended to other configurations which for example, employ more sophisticated optical arrangements to achieve tighter focus at the CCD, thereby increasing the experimentally

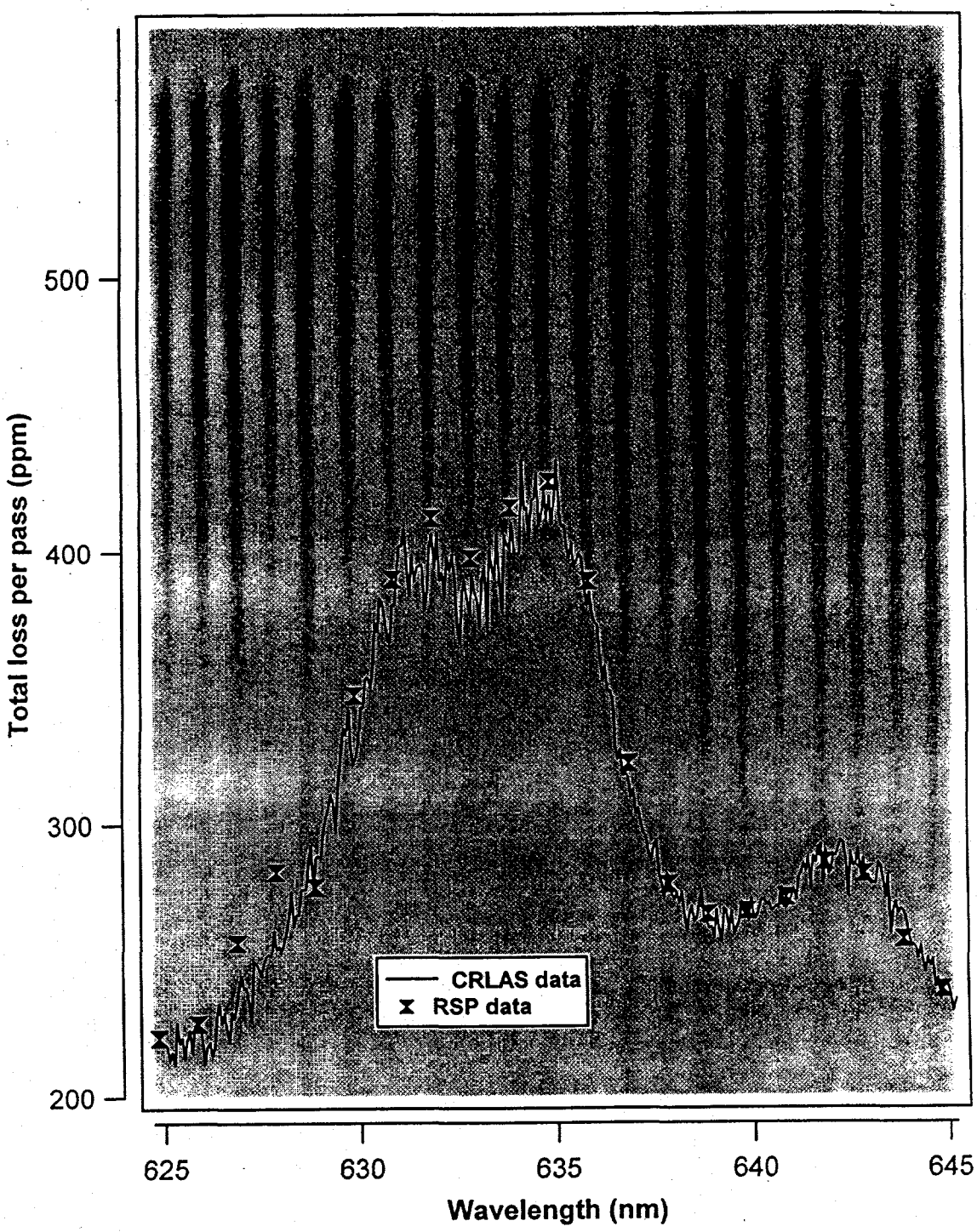

Figure 9. CRLAS and RSP overtone spectra of propane derived from fitting the corresponding individual streak traces. These data were obtained by scanning a narrowband dye laser in frequency, and subsequently measuring the spatial displacement of the individual streak traces. The extension of these studies suggests the same data can be obtained with a single pulse of broadband laser light, which would result in a continuous image.

achievable resolution. Below, we use the results of these initial experience to project performance levels of a more sophisticated RSP apparatus which employs a broadband light source together with higher resolving power extracavity optics. As discussed in the following Task, these RSP experimental results allowed us directly calculate the specifications required of the broadband light source for the Phase II prototype.

The initial scope of Task 4 in the Phase I research was to design the extracavity optical assembly for the Phase II apparatus, which is in a different spectral region from the above Phase I dispersion experiments. For this task, we targeted the 254 nm region, where strong absorption occurs for Hg as well as several other metals of specific interest to the DoE. In this spectral region, both ruled as well as holographic gratings are readily available. Here, we outline the design considerations for the specific case of a holographic grating, which, although less efficient (40% vs. 60% for ruled), results in much less stray light at the CCD. Gratings can be supplied from numerous vendors with a variety of line densities. One such grating measures 50x50 mm, with 2400l/mm (Edmund P43,226) and 40% efficiency, at a cost of ca. $220. If we illuminate the full 50 mm of the grating, we reach a theoretical resolving power of 120,000, which at 250 nm results in a resolution of .002 nm. Full illumination of the grating can be achieved by expanding the beam with cylindrical optics or beam expanding prism assemblies, as is commonly employed in laser oscillator design. However, as mentioned previously, the actual resolving power of the instrument will be limited by the effective slit width, which in the current case is theoretically limited by the 8 micron pixel size of each element of the CCD. The ability to achieve this degree of resolution will depend on the theoretical diffraction limit at the wavelength of interest as well as the (primarily spherical) aberrations of the focusing elements. The diffraction limit for a typical focusing element used above is ca. 5 microns, while the spherical aberration is ca. 10 microns. Other potential aberrations can further reduce the focusing ability, yet the expected levels will be in the 1-2 pixel size range. Based on these considerations, together with typical dimensions employed in these initial studies, we calculate an associated resolving power using the above grating (2400 lines/mm) of at least $4x10^4$. This, in turn, results in an instrumental resolution of .0065 nm at 250 nm, with the grating used only in first order.

This resolution is adequate for quantitative atomic spectroscopy of species such as Hg. Again, this figure can be improved by using higher orders, employing a larger format CCD with more or smaller pixels, or by using a grating with a higher line density. For studies above 300 nm, gratings with 3600 lines/mm are readily available, and will result in proportionately higher resolving powers. In some wavelength regions, it should also be possible to employ multiple grating assemblies (such as is commonly employed in visible dye lasers) to achieve resolving powers in the 10^6 regime. In the Phase II research plan, we again discuss the technical feasibility of developing a UV RSP instrument capable of resolving powers equal to or better than state of the art spectrophotometers and spectral analyzers, which are currently employed for quantitative analysis of chemical samples. In Phase II, we will explicitly model the limitations for a variety of configurations in order to achieve optimum performance for the target species.

Milestone of Task 4:

Task 4 successfully demonstrated the integration of the "streak camera" approach simultaneously with frequency dispersion at the cavity output. The fundamental principles of the RSP method were reduced to practice, using a relatively simple combination of off-the shelf hardware, and an absorption spectrum of propane was measured. The absorption intensities extracted from the RSP data were found to be in excellent agreement with those obtained with the well established CRLAS method, which exhibited lower levels of sensitivity than RSP for single-shot data. Preliminary design of the 250 nm region Phase II apparatus indicates that a UV instrument can be successfully constructed for the quantitative monitoring of atomic species, such as Hg.

Task 5. *Establish operating requirements of broadband laser source:*

In Task 5, we initially proposed to set-up and characterize a broadband light source, using a "modeless" dye laser at Sandia, in an effort to assess the feasibility of a broadband RSP apparatus. This "modeless" laser employs a series of beamsplitters and pump optics to amplify the light in a successive fashion with optical delays, resulting in a spectral output which lacks the sharp mode structure common to resonant cavity configurations. Standard resonant cavity configurations commonly result in large variations in output intensity as a function of bandwidth,

and we were initially not sure if this would pose a problem with the sensitivity and dynamic range limitations imposed by the camera. However, the insensitivity of RSP to variations in the spectral brightness of the light source evidenced in the phase I research indicated that this complex type of laser system was not necessary. Furthermore, the results of our research indicated that it was not necessary to actually construct a light source in order to reasonably assess the design specifications required for broadband operation. Additionally, the dye laser initially proposed was not configured for operation in the 510 nm region, which we have since targeted as the wavelength region of interest to the Phase II effort (for doubling to produce 254 nm light for Hg detection) As a result, we did not elect to use this system, and have begun construction of a simpler system which is described in detail in the Phase II Research Plan.

Briefly, an oscillator-amplifier dye laser system is being constructed for broadband operation in the visible, with subsequent doubling in a BBO crystal to produce broadband UV light. The results obtained above together with existing knowledge of doubling crystal technology were used to assess the power levels required for the development of such a light system for operation in the 254 nm region. Here, we present these analyses, which demonstrate that a simple broadband dye laser will produce adequate light for single shot measurements in the ultraviolet. By employing a more sensitive camera or on camera averaging, the requirements given below could be relaxed by roughly two orders of magnitude, which introduces the potential for the use of significantly smaller and less expensive solid state devices. Additionally, the laser system design which will be completed in Phase II can be easily configured for operation throughout the UV-vis regions, and therefore is capable of targeting numerous atomic as well as molecular species. The broadband light source specifications presented below are explicitly designed for single shot measurements employing cameras with the same sensitivities as that employed for the Phase I research. Employing cooled CCD arrays will result in a power requirement which is relaxed by more than an order of magnitude, taking into account requirements of the doubling crystal. Similarly, the ability to "on-camera" average, wherein data update intervals can be extended to a few seconds, will further reduce the requirements on the laser source. Here, we focus on existing, proven technology, to assess the feasibility of a UV

RSP instrument for primarily DoE related needs. Again, these projections build upon the results of the Phase I demonstrations above.

The single shot streak traces displayed in the previous sections were recorded with a laser energy ranging from 10-100 microjoules per pulse (measured just before the cavity), which in many cases was sufficient to saturate the pixels in cases where 7-20 pixels were illuminated in the vertical axis of the array. For the frequency dispersed data, wherein 7 pixels were illuminated, the first order light off of the grating was used, and was approximately 5 times weaker than the zero-order light. This grating was blazed for operation in the third order at 500 nm, and was not optimized for the current experiments in first order at 630 nm. Nonetheless, saturation of the camera pixels was evidenced with an input energy (at the cavity) of 50 microjoules per pulse. This same level of saturation will scale with the square of the spot radius, which if reduced to 1/3 of its current size will require only 1/9 of the 50 microjoules, or approximately 6 microjoules/pulse. We can use this figure to directly extrapolate the necessary spectral brightness of a broadband laser source, to determine the attainable spectral resolution and coverage for the Phase II apparatus. At this point it is important to note that the above saturation levels are determined with a mirror reflectivity of 99.99%, and will occur proportionally with the reflectivity. A reduction in mirror reflectivity to 99.95% would result in an associated 25 times reduction in the level of light required to saturate the camera pixels. It is also relevant to note that increased well depth CCD's can also be implemented, with associated changes in the saturation level.

The target wavelength for the eventual Phase II prototype will be 254 nm, specifically chosen for the ability to monitor mercury vapor, as well as several other species as presented earlier. If we assume similar response for the CCD at these wavelengths, and use the same ca 5 microjoule/pulse/unit bandwidth limit for saturation of the detector, we can easily compute the required power, depending on the target resolution and coverage. For the quantitative detection of atomic species at 254 nm, a resolution of ca. .005 nm is required, which translates into a resolving power for the extracavity optics of 5x104. If we use the requirement of 5 microjoules/.005 nm for the light source, we arrive at a total energy requirement of 1mJ/nm,

assuming we wish to fill the array with this same spectral coverage (i.e. ca. 200 frequency elements each of ca. 2 pixels). Assuming a conversion efficiency in a BBO crystal of 20% (typical at a spectral brightness of $10uJ/.1cm^{-1}$), this means we need a spectra brightness of 5 mJ/2 nm, or 25 mJ per 10 nm in the visible. This value, again, is based on a mirror reflectivity of 99.99%, which to date we have not seen at these wavelengths. We have, on the other hand, worked closely with a coating company who has produced a set of ringdown mirrors with a reflectivity of 99.96% at 254 nm. LGR currently possesses and commercially markets these mirrors, and will continue to work with the coating vendor on the development of higher reflectivity mirrors for UV studies. As a result, using the current mirror reflectivity of 99.96%, a saturation level at the camera will occur at UV wavelengths with a visible laser energy of ca. 4 mJ/25 nm, assuming a lower doubling conversion efficiency in the BBO crystal.

The above calculations indicate that RSP can be implemented with a broadband laser source of modest output powers, using the same standard CCD as that used in the Phase I research. As a direct consequence of the above analysis, the use of a larger array with more pixels will enable a larger spectral region to be covered with the same laser requirements, as the configuration will be limited primarily by the number of channels in the frequency axis, and not the bandwidth of the light source. Similarly, an increased camera sensitivity will result in significant reductions in the required spectral brightness of the input light source, which suggests new opportunities for a variety of solid state devices.

Milestones of Task 5.

The results of both the experimental data as well as the design analyses performed in Task 5 indicate that a broadband UV-vis RSP apparatus is technically feasible, using off-the-shelf components. The associated requirements on the broadband light source are found to be relatively modest, and additionally suggest that other light sources may be implemented by either using more sensitive, cooled CCD arrays (for UV studies), or by eliminating the need to frequency double (e.g. in visible or IR studies). Similarly, in cases where stronger absorption is expected (i.e. the sensitivity does not need to be a few ppm), the mirror reflectivity may be reduced, leading to reduced requirements on the broadband light source.

Task 6. *Sensitivity and spectral resolution*

In this task, the above results were used to determine the routinely achievable RSP sensitivity (fractional absorption) as well as spectral resolution. These analyses indicate that RSP can be implemented with a success greater than or equal to the performance of CRLAS systems, which have been proven to be robust in numerous environments, but to date are not capable of real time monitoring.

Sensitivity

The routinely achievable sensitivity limit for an RSP apparatus, based on the simple components used in the Phase I research effort, is derived from the demonstrated standard deviation of the fitted decay time constant. For the reflectivities used in these visible studies, which were 99.99%, the associated typical decay time uncertainty of 0.5% translates into a fractional absorption sensitivity of 5×10^{-7}. As mentioned in the data presented in Task 5, the decay time precision for the frequency resolved RSP data varied from 0.5% to 1.0% over a variation of laser intensity of approximately 400%, for a modest background level (typically 5%). Assuming these same levels of tolerance for the spectral brightness of a visible laser source illuminating the same 8-bit camera, we arrive at corresponding sensitivity levels of 1 ppm fractional absorption or better. This instrumental sensitivity translates into a sub ppb concentration level for many of the targeted metals listed in the RCRA, and a ppt level for Hg vapor. Of course, many of these species possess transitions in the ultraviolet, where high mirror reflectivity is more difficult to achieve. For the Phase II instrument, wherein we target the 254 nm region for Hg detection, the expected level of performance is at least ca. 4 ppm fractional absorption sensitivity per pass, using the existing 99.96% mirrors. For the specific application of Hg detection at 254 nm, the corresponding concentration detection limit is ***30 ppt***! Increases in mirror reflectivity at this wavelength, which are specifically budgeted in the Phase II effort, will lead to comparative gains in sensitivity for the UV RSP apparatus.

An exciting note in this discussion is the recent availability of ultra high reflectors in the visible and IR. LGR currently markets and sells mirrors with reflectivities as high 99.9985%, as

a result of our close diagnostic work with several coating vendors. For these reflectivities, given the same uncertainties in the decay time, sensitivity levels in the 10^{-8} range can be achieved, with associated concentration detection levels in the ppt region for many atomic as well as molecular species. Of course, the use of mirrors of this quality will likely require the use of low temperature CCD elements, as the available light at the camera is a function of the square of the single mirror reflectivity. Nonetheless, this requirement again poses no major barrier with existing off-the-shelf hardware for many spectral regions. For the purposes of the Phase II UV development, we expect a routine sensitivity of 2-3 ppm fractional absorption sensitivity at 254 nm. In Task 7, we used these data to extrapolate detection limits for several RCRA-targeted metals.

Spectral resolution

As discussed above, the single-shot spectral resolution and coverage achievable is a function primarily of the extracavity optical assembly and camera dimensions, as the laser system will produce a pulse of light which is likely broader than the desired spectral coverage. The specific RSP application of metal detection via the associated atomic spectra requires an instrumental linewidth which is close to the transition linewidth for the source implemented. This required linewidth includes contributions from Doppler as well as pressure broadening, in addition to the natural or lifetime broadened linewidth. In cases where direct calculation of the concentration is desired from the absorption spectra, the instrumental linewidth should be at least as narrow as the total transition linewidth, including the above contributions. In cases where the instrumental linewidth is broader than the transition linewidth, concentrations can still be deduced from the absorption spectra, but with a lower sensitivity, which to first order scales with the ratio of the associated linewidths. In this section, we again highlight the achievable instrumental linewidth and resolution in the UV, and in Task 7 translate this figure into species concentrations assuming an ICP source is employed, which effectively atomizes all species in the stream to determine total elemental concentrations

In Task 4, we estimated an instrumental resolving power of 4×10^4, based on modest requirements of the extracavity optics with associated focusing limits, etc. This figure is based

on a grating-to-camera distance of ca. 20 cm, which directly effects the linear (vertical) displacement of the light as a function of frequency. This displacement can be increased to several times this value, with roughly proportionate increases in the linear displacement, and hence, resolution, as is commonly achieved in monochrometers. We expect that for high resolution studies, the resolution limit will be approximately $1x10^5$, using a single 10 cm grating with 2400 lines/mm in first order, and a grating to camera distance of <1 m. Again, this figure could be increased by simply using the grating in second order, but here we will use this $1x10^5$ value in the following analyses. Of course, in RSP, there is a compromise between wavelength coverage and resolution, as with any frequency selective instrument.

The spectral coverage achievable at a resolving power of 10^5 will be determined by the number of pixels illuminated per wavelength interval (dictated by focusing) times the total number of pixels in the array. Using the 2-pixel figure given above for the focusing limit (dictated by spherical aberrations) together with a 1000x1000 pixel CCD array, a coverage of 5 angstroms at 250 nm results. This resolution and coverage is more than adequate for quantitative atomic studies, and will allow nonresonant contributions to the total cavity losses to be determined in addition to the losses due to absorption. This ability is absolutely essential for rapid assessment of species concentrations, and is currently not possible with conventional CRLAS, which must be scanned in frequency. Extrapolation of the above analyses to include larger array sizes or lower resolution scans in completely straightforward. For example, the single-shot wavelength coverage given above will scale linearly with the number of elements in the array, and with the pixel diameter. For a 25 micron pixel size, single pixel resolution will be possible, which when combined with a state of the art 4000x1000 CCD array will yield a (single shot) scanning capability of a full 4 nm at a resolution of 2.5 pm. This, in turn would enable the potential ***simultaneous*** detection of Hg, Fe, Co, and Ti, which have transitions in between 252 and 254 nm.

The above analysis can similarly be applied to the detection of molecular species, which in many cases will exhibit broad spectral features. In this case, it is simple to configure the RSP instrument for broad scans at lower resolution. For example, 20 nm could be covered at a

resolution of .02 nm with a 25 micron pixel 1000x1000 CCD array. These bandwidths are currently achievable with a single set of high reflectivity mirrors in the UV, while in the visible, bandwidths are typically 15% to 20% of the design wavelength. In practice, the RSP method will prove to be compatible with existing, off-the-shelf hardware, as well as capable of performing at levels required for quantitative spectrometric measurements. Below, we outline the detection limits associated with the detection of specific heavy metals, when RSP is used in conjunction with an inductively coupled plasma source (ICP). In Phase II, we will explicitly demonstrate this capability by integrating our RSP prototype instrument with an ICP source, in a collaborative effort with Drs. G.P. Miller and C.B. Winstead at Mississippi State University, who have been performing conventional CRLAS measurements on ICP sources for the DoE. A letter of interest and intent from these researchers is included at the end of this proposal.

Milestones of Task 6.

The results of the analyses performed in Task 6 of the Phase I research indicate that resolving powers of $1x10^5$ can be routinely achieved in an RSP instrument, with an associated absorption sensitivity of <1 ppm in visible and <4 ppm in UV spectral regions (250 nm), respectively. These performance specifications are adequate for quantitative studies of ultra-trace metals and molecular species, with sensitivity levels exceeding many state of the art techniques by orders of magnitude.

Task 7. *Concentration detection limits*

For Task 7, the sensitivity values as discussed in Task 6 are used to calculate concentration detection limits for several species of interest to the DoE. Specifically, we focused on heavy metals which are targeted in the RCRA. In this Task, we placed special emphasis on the detection of heavy metals via a combination of UV RSP and an ICP source, as we plan to actually test the RSP method in an ICP source as part of the Phase II effort, as a collaborative effort with the group at Mississippi State University. However, here we also present some detection limits for species with visible transitions, which could similarly (and more easily) be monitored. Following the formalism presented earlier in Section 4, the absorption cross sections are calculated from the product of the lineshape functions and associated linestrengths. Here, we

present the resulting cross sections for the Doppler-broadened cross sections, which typically dominate spectral features in ICP sources. These data are then combined with the expected path length within the ICP source to calculate concentration detection limits. The data are additionally converted to expected sensitivities for solution phase concentrations of these same metals, in order to directly compare with sensitivity levels obtained with currently employed analytical methods, which combine ultrasonic sample nebulatization with ICP-MS and ICP-atomic fluorescence (AFS) studies. The associated gas phase detection limits for non-solution prepared samples are significantly higher than the values given below. Again, here the $4x10^{-6}$ fractional absorption limit calculated above for the 250 nm region is used throughout, although many of these transitions lie in regions where the mirror reflectivities are significantly higher. In these cases, the expected performance level will increase exponentially with the better reflectivities, which is not taken into to account in the below data.

In Table 2, we present detection limits for the associated species for the RSP- ICP instrument, as discussed above. Here, an ultrasonic nebulized sample efficiency (ppb=2.5xugm^{-3}) was estimated to determine solution detection limits in the ppb range. These data are presented as both ppb as well as ugm^{-3}, for an ICP source with an effective path length of 5 mm. As seen in the Table, the detection limits for nearly all species are in the sub-ppb level, even for the very weak Cd transition at 326.1 nm. These data indicate that RSP should be capable of easily exceeding the 5 ug/m^3 detection limits sought by the DoE, and as proposed by the EPA. The strong Cd transition is expected to have detection limits at the ppt level, which even if predicted to be overly optimistic by an order of magnitude, is on the order of ICP-MS systems, which typically cost several hundred thousand dollars. The detection limits are also similar to those demonstrated by ICP-AFS studies, which probed species roughly 20 mm above the ICP coil.[20] The below detection limits predicted for an RSP instrument of modest performance (4 ppm), indicate that the technology is suitable for the real-time monitoring of ultra trace level concentrations of heavy metals. When used in conjunction with an ICP, RSP can determine total elemental concentrations in the offgas, as the source can be optimized for efficient atomization. Miller and Winstead[21] have recently demonstrated the successful implementation of conventional

CRLAS with an ICP source, which suggests that the extension of RSP to ICP sources is possible and should pose no significant barriers.

Element	wavelength (nm)	mass (amu)	linewidth (pm)	cross section	detection (ug/mm^3)	detection ppb (soln)
Cd	228.8	112.4	1.5	$4.4x10^{-12}$	$3.4x10^{-4}$	$8.6x10^{-3}$
Cd	326.1	112.4	3.0*	$6.1x10^{-15}$	0.243	0.63
Hg	253.6	200.6	3.8	$3.7x10^{-14}$	0.113	0.28
Pb	283.3	207.2	2.1	$7.3x10^{-13}$	0.0059	0.015
Ti	377.5	204.4	2.7	$6.2x10^{-13}$	$4.4x10^{-3}$	0.011
Al	394.4	27.0	5.0*	$3.2x10^{-13}$	$1.16x10^{-3}$	$2.8x10^{-3}$
Mn	403.1	54.9	6.2	$1.4x10^{-14}$	$5.1x10^{-4}$	$1.3x10^{-3}$
Cr	425.4	52.0	3.8	$4.6x10^{-13}$	$1.5x10^{-3}$	$3.7x10^{-3}$
Cs	455.5	132.9	3*	$7.2x10^{-13}$	$2.4x10^{-2}$	$2.6x10^{-6}$
Sr	460.7	87.6	3.8	$9.9x10^{-12}$	$5.9x10^{-4}$	$2.9x10^{-2}$
Cs	852.1	132.9	3*	$1.7x10^{-11}$	$1.1x10^{-4}$	$2.6x10^{-4}$

* estimated linewidths

Table 2: Detection limits predicted for an RSP apparatus when used in conjunction with an ICP source. These limits are converted to liquid sample concentration values, in order to compare with currently implemented methods.

Milestone of Task 7:

Task 7 predicts that RSP will be capable of detecting heavy metal concentrations for a variety of species targeted in the RCRA at the sub-ppb level, based on the cumulative results of the above Tasks.

Summary of the Phase I Research:

The Milestones achieved in the course of the Phase I research constitute the successful achievement of the Phase I Objectives. Furthermore, the demonstration of simultaneous frequency dispersion together with the streak camera principle was achieved, yielding the first RSP absorption data (of propane). This specific Task was initially slated for the Phase II effort.

The collective results of the Phase I research indicate that the RSP method should be capable of real-time monitoring of chemical species with extremely high sensitivity, combined with unparalleled effective scanning speed. The ability to monitor species concentrations via their associated absorption spectra will have numerous applications ranging across commercial as well as research venues. The unique ability of RSP to determine absolute species concentrations in microsecond timescales can be exploited for other uses beyond those focused on here, such as the kinetic study of reactive species. The demonstrated sensitivity levels evidenced in the Phase I research additionally indicate the potential for a commercially viable analytical instrument, as the components employed were inexpensive, off-the-shelf items (with the exclusion of the laser system used in these studies). The proposed Phase II Project outlined below focuses on further developing and refining the Phase I instrument to produce a broadband prototype. Additionally, the adaptation of RSP for use with an ICP source in collaboration with the group at Mississippi State University (MSU) is proposed. This group has successfully demonstrated the adaptation of CRLAS for metals detection in the UV employing ICP sources for atomization of metal-containing compounds, and possesses expertise in the operation of such sources. We plan to combine our RSP Phase II prototype instrument with ICP sources provided by the MSU group to demonstrate the ultra-trace-level detection of metals, to verify the associated detection limits projected above. A letter of from the MSU group is included in this proposal.